Chaperones and Chaperone–Substrate Complexes:

Dynamic Playgrounds for NMR Spectroscopists

Björn M. Burmann, Sebastian Hiller*

Biozentrum
University of Basel
Klingelbergstrasse 70
4056 Basel
Switzerland

*Corresponding author. Tel.: +41 61 267 20 82; fax +41 61 267 21 09

E-mail address: sebastian.hiller@unibas.ch

Abstract

The majority of proteins depend on a well-defined three-dimensional structure to obtain their functionality. In the cellular environment, the process of protein folding is guided by molecular chaperones to avoid misfolding, aggregation, and the generation of toxic species. To this end, living cells contain complex networks of molecular chaperones, which interact with substrate polypeptides by a multitude of different functionalities: transport them towards a target location, help them fold, unfold misfolded species, resolve aggregates, or deliver them towards a proteolysis machinery. Despite the availability of high-resolution crystal structures of many important chaperones in their substrate-free apo forms, structural information about how substrates are bound by the chaperones and how they are protected from misfolding and aggregation is very sparse. This lack of information arises from the highly dynamic nature of chaperone–substrate complexes, which so far has largely hindered their crystallization. This highly dynamic nature makes chaperone–substrate complexes good targets for NMR spectroscopy. Here, we review the results achieved by NMR spectroscopy to understand chaperone function in general and details of chaperone–substrate interactions in particular. We assess the information content and applicability of different NMR techniques for the characterization of chaperones and chaperone–substrate complexes. Finally, we highlight three recent studies, which have provided structural descriptions of chaperone–substrate complexes at atomic resolution.

Contents

1 Introduction

Cells in all kingdoms of life rely on functional proteins. To ensure that all proteins obtain their right fold and functionality at the right time at the right place, cells rely on intricate chaperone and protease systems [1, 2]. These machineries ensure proper folding, and at the same time are crucial for the prevention of the deleterious effects of protein misfolding and aggregation, that might lead in the end in cell death, in neurodegeneration and in other protein misfolding diseases [3, 4]. A set of diverse protein families termed molecular chaperones assists a large variety of processes involving folding, translocation, unfolding, disaggregation and homeostasis of proteins within the cellular environment [3, 4]. Despite being essential for cell survival, chaperones are not prototypical macromolecular machines with well-defined substrate specificity. Chaperones usually feature broad specificity to engage a large variety of substrates [1, 2]. The different roles of chaperones lead to a network of folding assistants, which can act in ATP-dependent or ATP-independent manner to protect substrates from engagement in non-productive folding pathways. Chaperones often interact with their substrates in a highly dynamic manner, due to the inherently disordered nature of unfolded and partly folded substrate polypeptides. This inherent flexibility of the substrates has so far prevented the structure determination of chaperone–substrate complexes by X-ray crystallographic studies. On the other hand, this flexibility makes such complexes suitable targets for NMR spectroscopy, which in recent years became applicable to large protein sizes through advanced techniques such as specialized labeling schemes and methyl TROSY spectroscopy [5-7].

The aim of this work is to review the multiple contributions of NMR spectroscopy to the understanding of structure, dynamics and function of molecular chaperones and their complexes with substrates. In this discussion we include also studies on large protease machineries, since these have similar structural biology with respect to handling unfolded substrate polypeptides and since they – although technically they are not chaperones – contribute to cellular protein homeostasis. Section 2 introduces the known chaperone functions in their biological context. Section 3 discusses the impact of different NMR techniques in characterizing chaperone systems. Section 4 summarizes published NMR studies of chaperone systems that have contributed to understanding structure, function and dynamics. As a synthesis of these studies, section 5 assesses the role of NMR studies to elucidate the two adaptation mechanisms of chaperones towards their substrates. Finally, section 6 reviews available structures and structural models of chaperone–substrate complexes at atomic resolution.

2 Chaperone functions

The classical *in vitro* experiments on the renaturation of ribonuclease by Anfinsen established the dogma that protein structure is encoded in the amino acid sequence [8], which is true even for proteins that can adopt two fundamentally different conformations [9-11]. *In vitro*, protein folding thus results from the self-assembly of an unfolded polypeptide chain to a conformation of low free energy. *In vivo*, however, protein folding requires in many cases additional control by helper proteins, the molecular chaperones [12, 13]. A chaperone is a protein that is necessary for the biogenesis of a substrate protein, but that is not part of the final stable fold of the substrate [14-17]. Functionally, chaperones interact with unfolded polypeptide segments to prevent aggregation and release their substrates in a non-aggregation-prone state, often coordinated with the synthesis rate and folding speed of the substrate [14, 17]. Molecular chaperones form a cellular network of small proteins involved in accompanying and supporting newly synthesized proteins on their way to their functional structure and its functional environment (Figure 1A and Table 1).

2.1 Holdase chaperones

Chaperones with holdase function bind unfolded or non-natively folded segments of substrate polypeptides for sufficient long life times that the substrate can be translocated across a membrane or an aqueous environment, or can be synthesized to completeness prior to adopting its native fold [16, 18]. An important mechanistic aspect of the holdase function is its energy-independence. Holdase chaperones thus can influence the folding of their substrates only passively, e.g. by protecting them against aggregation. Holdase chaperones interact with their substrates at different stages of protein biogenesis. For example, bacterial trigger factor binds directly to the ribosome in close proximity to the exit channel and can thus directly protect the emerging nascent polypeptide from aggregation during synthesis and enable subsequent folding [19-22]. Other important holdases are the periplasmic chaperones Skp and SurA, which deliver integral outer membrane proteins (Omps) to their final destination, the outer membrane [23].

2.2 ATPase chaperones

Some chaperones feature an ATPase function, which allows them to interfere with the folding process of their substrates in an energy-dependent manner. Such chaperones interact with unfolded or misfolded substrates and use cycles of ATP consumption to facilitate substrate folding [24]. ATP hydrolysis provides the energy for allosteric changes into the chaperone structure to help substrate proteins reach their native and functional fold [25]. In addition, some

of the most ubiquitous ATPase chaperones, such as Hsp70 and Hsp90, use a plethora of auxiliary co-chaperones to modulate their function [18, 24, 26]. Importantly, direct coupling of the ATPase activity to substrate folding has so far not been established for all ATPase chaperones [25]. For example, while the functional details of the folding mechanisms of Hsp70 and Hsp90 are not fully known, current models suggest that ATP-dependent structural rearrangements of the chaperones lead to substrate release, facilitating the substrate to fold into its native state or rebind the chaperone [27].

2.3 Chaperonins

Chaperonins are a special subgroup of ATPase chaperones with large double-ring complexes. Chaperonins are divided in two subgroups: Class I chaperonins are found in bacteria, mitochondria, and chloroplasts, forming heptameric ring structures, and associate with smaller Hsp10-proteins (GroES in bacteria) that form the lid-element of the folding cage. Class II chaperonins in Archaea and the eucaryotic cytosol form octa– or nonameric ring structures, containing a built-in protrusion structure forming a lid [28]. Functionally, both classes have in common that they fully encapsulate their respective substrates in their folding chambers and drive the substrate protein in an energy-dependent manner towards its native fold [29]. The GroEL/ES chaperonin has been studied extensively (reviewed e.g. in [29, 30]), and it has been shown that many GroEL-dependent proteins exhibit complex protein folds relying on many long-range interactions [31, 32], leading to a high tendency to populate kinetically trapped folding intermediates [33]. Binding of the lid domain GroES is preceded by binding of ATP to GroEL and induces large conformational changes within the GroEL folding chamber, leading to the exposure of the highly hydrophilic, net negatively charged, inner wall [34].

2.4 Unfoldases

Chaperones with unfoldase function interact with folded or misfolded substrate proteins and unfold these under the consumption of ATP. Clp (Hsp100) proteins are homohexameric AAA+ (ATPases associated with diverse cellular activities) ring-shaped unfoldases. These proteins bind preferentially to an exposed peptide tag, the small and stable 11-residue 10S RNA ssrA-tag, on their substrates, that target them to the ClpA and ClpX unfoldases [35]. The proteins thread their substrates through their inner pore, lined with Tyr residues on mobile pore loops providing the binding sites for translocating chains, without specificity for sequence or chain polarity [36]. The unfoldase uses channel rotations induced by ATP hydrolysis once a polypeptide loop or terminus is engaged within the inner pore to use a translocation-coupled unfolding mechanism to unfold their substrates [37-39]. A crystal structure of an asymmetric

ClpX ring shows a sequence of pore loops at different heights with an axial separation of 1 nm [39], which is in excellent agreement with optical-tweezer experiments indicating 1 nm translocation steps [40, 41]. These unfoldases interact directly with the ClpP protease for subsequent protein degradation [35]. Another example of an unfoldase is DnaK (Hsp70) of *E. coli* [27], which works without an associated protease and leads to the folded state of the substrate. Recently, it was shown that DnaK uses the energy generated by ATP hydrolysis to expand and therefore unfold misfolded polypeptide chains [42] before it releases these to fold back to their native states [27].

2.5 Disaggregases

Some specialized proteins of the Hsp100-class (ClpB in bacteria, Hsp104 in yeast) have the ability to resolve existing protein aggregates in an ATP-dependent manner [43, 44]. Structurally, these proteins are hexameric proteins consisting of two ATPase domains, which are divided by a 90 Å long coiled-coil propeller [45]. ClpB couples its unfoldase and disaggregase function to the Hsp70-system [46]. Binding of the Hsp70 ATPase domain to one end of the coiled coil, a region highly sensitive to mutations, is essential for disaggregation [47, 48]. In the current model for the synergistic action of ClpB and DnaK, the DnaJ-protein initially interacts with the aggregate and mediates the binding of the substrate to DnaK [49-51]. Subsequently, DnaK might use its unfoldase function to loose some exposed unstructured regions [27], before it recruits the ClpB-disaggregase [46, 50, 52]. Upon aggregate engagement the disaggregases extract polypeptides from the aggregate and unfold them by forced translocation through their central pore [46, 53-55]. ClpB/Hsp104 are able to employ the protein-translocation mechanism described above for the unfoldases [35]; this possibility was elegantly demonstrated by engineering ClpB and Hsp104 to allow them to bind the ClpP protease and then showing that these multiprotein complexes functioned as degradation machines [46, 53].

2.6 Translocases

Transport of proteins across membranes requires a special class of chaperone, the integral membrane translocases (Figure 1B). Translocases are structurally either α-helical membrane proteins that transport pre-proteins across the bacterial cytoplasmic membrane, the eukaryotic endoplasmic reticulum, or the mitochondrial inner membrane [56, 57], or alternatively they are β-barrel proteins embedded in the outer membrane of Gram-negative bacteria, mitochondria, or chloroplasts [23, 58]. Despite their structural divergence, these proteins share the translocation function for unfolded or partly unfolded pre-proteins across the respective membranes. Whereas the bacterial SecYEG-complex uses auxiliary proteins to generate the energy needed by

ATP consumption in concert with the proton motive force (reviewed in [59]), integral β-barrel proteins like Tom40 in mitochondria [58], Toc75 in chloroplasts [60], and FhaC in Gram-negative bacteria [61] rely solely on a thermodynamic gradient to translocate proteins, with possible contributions from substrate protein folding. The details of the translocation mechanism for these proteins remain elusive.

2.7 Insertases

Insertion of integral membrane proteins into the membrane is catalyzed by insertase chaperones, which can be of either α-helical or β-barrel secondary structure. SecYEG-protein mediated membrane insertion into the bacterial inner membrane is achieved by lateral gate opening and insertion of complete membrane spanning helices into the adjacent membrane [62]. Depending on the different membrane proteins either the SecYEG or the YidC insertase can either independently or together facilitate membrane insertion (reviewed in [63]). The mechanism for the insertion of β-barrel membrane proteins remains less clearly understood. Recently, several high-resolution crystal structures shed new light on the functional aspects of membrane insertion. The crystal structures of BamA [64-66] and its homologue TamA [67] revealed that in the BamA/TamA barrel the contact between the last and the first strand is weakened and can provide a lateral gate towards the membrane. Based on this observation hybrid-barrel [67, 68] and membrane distortion models [64, 69] for membrane insertion were proposed.

2.8 Proteases

Large protease machineries are a part of the overall cellular protein homeostasis machinery, although technically they are not chaperones. Nonetheless, their structural biology with respect to handling unfolded substrate polypeptides has many similarities to that of chaperones, and the applications of NMR spectroscopy to study these systems is equally promising. The degradation of misfolded substrate proteins in cells relies on ATP-powered proteolytic machines (Figure 1C) [35, 70]. These proteases employ different active sites for the cleavage of the peptide bond: whereas the ClpP protease uses a His-Asp-Ser triad, bacterial HslV and the archaeal 20S peptidase of the proteasome use an N-terminal Thr as the active site nucleophile [71-74]. All these proteases form large multisubunit complexes of multilayered ring structures consisting of hexameric or heptameric rings stacking on each other to form cylindrical structures [72, 73, 75]. The proteolytic chambers are deeply buried inside these particles and are accessible to unfolded proteins only through channels that thus prevent inappropriate protein degradation [76, 77]. Unfolding occurs in the case of HslV with the associated HslU-unfoldase, for ClpP with the

associated unfoldases ClpX and ClpA, and for the 20S peptidase with the 19S core particle, which all use ATP-hydrolysis to translocate the unfolded polypeptides into the proteolytic chamber of the compartmental proteases [72, 78-80]. Once the unfolded polypeptide reaches the proteolytic sites, it is hydrolyzed into 3–30 amino acid long peptides [81-83].

3 NMR techniques for chaperone systems

This section reviews the impact of different NMR techniques on the characterization of chaperones and chaperone–substrate interactions. Importantly, the usefulness of the individual methods depends on the interaction mode between chaperone and substrate. Two fundamentally different interaction modes can be distinguished (Figure 2): i) The chaperone recognizes a certain segment of the substrate and binds it in a single, well-defined conformation. The resulting structure follows the biophysics of a conventional protein–protein interaction and classical NMR technology can be used for its characterization, including structure determination. ii) The chaperone binds its substrate as a conformational ensemble. The ensemble can bind tightly to the chaperone, although the individual local binding interactions are short-lived and rather weak [84, 85]. In this case, NMR techniques developed for dynamic ensembles are appropriate.

3.1 Chemical shift perturbation

Measurement of chemical shift perturbations (CSP) is a valuable method for the characterization of classical protein–protein and protein–ligand interactions [86, 87]. The approach quantifies the differences in chemical shifts between two states of a protein, typically the apo and the holo state. The chemical shift perturbations induced by close spatial contacts and direct conformational changes can be large in magnitude, and localize around the ligand-binding pocket or at the protein-binding interface. In addition, allosteric effects resulting from indirect conformational changes of the protein are typically observed distant from the binding pocket or interface [88, 89].

For chaperones with a substrate bound in a single conformation, the method of chemical shift perturbation is readily applicable and can be used to identify the binding interfaces [90, 91]. *For chaperones with a substrate bound in a dynamic conformational ensemble,* chemical shift perturbations are less straightforward to interpret. The CSP effects caused by direct interactions will average over multiple substrate conformations and thus have a tendency to vanish. Even for residues in direct contact with the substrate ensemble, the population-weighted averaging will result in only small chemical shift changes relative to the apo form. Allosteric changes, that are

of similar magnitude and sign for multiple conformations are, in contrast, retained in the average, but they may not be located at the interaction surface. Overall, the interpretation of CSP results cannot be expected to yield the binding interface in the ensemble situation. *When applied to substrates in equilibrium between a soluble and chaperone-bound form,* CSP can facilitate the identification of the interacting segments of the substrate polypeptide [86, 90].

3.2 Nuclear Overhauser effect and saturation transfer difference

The nuclear Overhauser effect (NOE) is the classical method to obtain intermolecular contacts in biomolecular complexes, and is the cornerstone of protein structure determination by NMR [92]. The NOE transfers magnetization *via* the dipolar coupling through space between two nuclear spins. Saturation transfer difference (STD) is a derivative of the NOE, using the additional effect of spin diffusion to map binding interfaces [93].

For chaperones with a substrate bound in a single conformation, measurement and interpretation of the NOE follows the practice established for folded proteins. The NOE can thus be used to calculate structures of chaperone–substrate complexes [91]. *For chaperones with a substrate bound in a dynamic conformational ensemble,* intermolecular NOEs can be observed, but their interpretation in terms of interspin distances is not straightforward, since the obtained intermolecular contacts are ensemble-averaged [85]. The NOE can thus not be converted into upper limit constraints for structure calculation. But the substrate interaction surface can be mapped – the NOEs of those residues that are in significantly close contact to the substrate for a significant proportion of the time average [85]. *For substrates in equilibrium between a soluble and chaperone-bound form,* STD can be fruitfully applied to localize the polypeptide segments in close contact with a large chaperone [94].

3.3 Paramagnetic relaxation enhancement and pseudo contact shift

Measurement of paramagnetic relaxation enhancements (PRE) and pseudo contact shifts (PCS) are well-established for intermolecular measurements in protein–protein and protein–ligand complexes [95-97]. For this method, a paramagnetic moiety, typically a lanthanide binder or an organic radical, is chemically attached to one of the proteins. The paramagnetic effects on the relaxation or the chemical shifts are then detected on the nuclei of the second protein or the ligand. The resulting PRE effects can be converted into interspin distance constraints, which may be used in structure calculations. The strong paramagnetic relaxation enhancement allows for measurements of large distances in the 10–25 Å range [98, 99]. The PCS can be converted into orientational constraints [100, 101]. Importantly, the PRE is highly sensitive to states with low

populations, and consequently, it has been successfully applied to conformational ensembles [99].

For chaperones with a substrate bound in a single conformation, application and use of the PRE and the PCS is straightforward and follows the techniques used for classical proteins [102]. *For chaperones with a substrate bound in a dynamic conformational ensemble,* when suitably arranged, triangulation with PREs allows the calculation of spatial areas around the chaperone that are populated by the dynamic substrate [84]. Use of PREs may be the method of choice, since it allows the mapping of contacts in the ensemble in a sensitive but still atomically-resolved way. PCS applications to chaperone–substrate complexes have so far not been reported. It can be expected that the PCSs should be able to detect residual non-random orientation of the substrate within the chaperone.

3.4 Measurements of spin relaxation parameters

Measurements of spin relaxation parameters are generally a highly important method for characterizing protein dynamics [103]. Various different approaches are in use, including measurements of backbone nitrogen nuclei and relaxation dispersion. *For chaperones with a substrate bound in a single conformation,* backbone dynamics give information comparable to folded proteins. *For chaperones with a substrate bound in a dynamic conformational ensemble,* backbone dynamics have been used to highlight the ensemble character of the substrate in fast exchange [84]. Methods for spectral density mapping that had originally been developed for unfolded protein ensembles were successfully applied [84, 104]. Measurements of relaxation parameters can highlight the fast dynamics observed and detect substructures of the conformational ensembles [104]. *For substrates in equilibrium between a soluble and chaperone-bound form,* relaxation-dispersion measurements have been used to quantify the kinetic off-rate constants [91, 105, 106].

3.5 Dark state exchange saturation transfer

Very large, or immobile, assemblies of biomolecules feature broad resonance lines and are thus not observed in solution NMR experiments. These assemblies have consequently been termed “dark states”. Dark exchange saturation transfer (DEST) exploits the substantial quantitative differences in relaxation rate constants between a soluble form of small overall size and a dark state [107, 108]. For chaperone–substrate systems, the method is thus favorably applied in equilibrium situations where a soluble protein is in fast exchange with a chaperone-bound form that is otherwise inaccessible to NMR spectroscopy. DEST can thus identify the contact regions of the substrate. The method has been applied in the case of GroEL [109].

3.6 Hydrogen/deuterium exchange

Amide proton exchange rates can be quantified by measurement of the disappearance of amide group signals after transfer of the sample from H_2O into D_2O. This hydrogen/deuterium (H/D) exchange method is generally very helpful for characterizing proteins and it can provide insights into chaperone–substrate complexes in cases where parts of the substrate feature residual structure [110]. So far, H/D exchange has been applied to chaperone–substrate complexes to obtain insight into the chaperone-dependent alteration of the folding trajectories of substrate proteins [111-113].

3.7 Solid state NMR spectroscopy

Solid state NMR spectroscopy under magic angle spinning is a method of choice for the characterization of large protein systems [114, 115]. For the application to chaperone–substrate systems, ssNMR may be a useful method, when the complexes are long-lived. This may be of interest in connection with the sedimentation/FROSTY method, where the chaperone is spun down [114, 116, 117]. While ssNMR has been applied to study the apo forms of large chaperones [115, 118], this method awaits application to chaperone–substrate complexes.

3.8 Residual dipolar coupling

Measurements of residual dipolar couplings (RDCs) are generally employed to determine orientations of internuclear vectors relative to a frame of reference, the alignment tensor, which is provided by partial orientation of the biomolecules [119, 120]. *For chaperones with a substrate bound in a single conformation,* this method can be applied as for folded proteins and will provide additional constraints for structure calculations. *For chaperones with a substrate bound in a dynamic conformational ensemble,* the application would be of particular interest, since the well-folded chaperone and the substrate ensemble will be aligned with the same tensor. The alignment tensor was determined from the data of the well-folded chaperones and the method could thus for instance detect the existence of residual alignment of the substrate ensemble [119, 120]. So far, however, RDCs have only been measured for chaperones in the apo state and not for chaperone–substrate complexes [121-123].

4 Chaperone systems characterized by NMR spectroscopy

4.1 Trigger factor

The first chaperone to interact with a nascent polypeptide chain in bacteria is the ribosome-bound trigger factor [20, 124]. Structurally, trigger factor is a three-domain protein containing a ribosome-binding domain (RBD), a substrate-binding domain (SBD), and a peptidyl-prolyl-isomerase domain (PPD) [19, 125], which links trigger factor to the classical foldases [126]. *In vivo*, substrate-free trigger factor undergoes a three-state equilibrium involving a monomeric and a dimeric form, and a monomeric ribosome-bound form [127]. Ribosomal profiling experiments have revealed that outer membrane β-barrel proteins are highly abundant among trigger factor substrates *in vivo* [128].

The first reported NMR study of trigger factor was the determination of the solution structure of PPD from *M. genitalium*, revealing a classical FKBP (FK506 binding protein) fold, consisting of four antiparallel β-strands and two adjacent α-helices [129, 130]. Subsequently, an X-ray structure of the RBD revealed an elongated α + β structure consisting of a four-stranded antiparallel β-sheet flanked by two long α-helices that forms a dimer [131]. An analysis of the RBD in solution indicated that this domain also exists as a dimer in solution, and the secondary chemical shifts showed good agreement with the secondary structure elements observed in the crystal structure. However, the third β-strand at the edge of the β-sheet was found to be disordered in solution [132]. Full-length X-ray structures of trigger factor showed different asymmetric dimers [19, 125, 133], which interestingly did not dimerize *via* the RBD. To address the differences between the reported crystal structures, the Dyson group analyzed the secondary structure elements thoroughly with a trigger factor construct lacking the RBD, which appeared monomeric in solution [134]. Analysis of the secondary structure of the trigger factor construct lacking both RBD and PPD showed good agreement with the published structures from *E. coli* and *T. maritima* [19, 133]. Despite this good agreement of secondary structure elements, RDC measurements could not be brought into consistency with the X-ray structure, which may be explained by a yet different conformation in solution, or by conformational heterogeneity [134]. The latter might be further evidenced by the additional observation that this region of the protein is highly flexible on a number of different timescales, as shown by relaxation measurements [134]. Recently, the Kalodimos group determined the structure of trigger factor in complex with its substrate alkaline phosphatase (PhoA) [91]. By using chemical shift mapping, intermolecular NOEs, and ITC measurements, it was shown that trigger factor contains four distinct binding sites with different affinities for diverse PhoA-peptides [91]. The data thus showed that the peptides are able to subsequently bind to different binding sites, as

would be the case for the ribosome-bound-state of trigger-factor, when it engages the constantly elongating nascent chain [20, 91, 124].

4.2 DnaK/DnaJ (Hsp70/Hsc70/Hsp40)

The most abundant chaperone in pro- and eukaryotes is Hsp70 (DnaK in *E. coli*), which exists as many orthologues in different cellular compartments. Hsp70 carries out a wide diversity of functions, including protein folding, translocation across membranes, and disaggregation of aggregates, with the help of a large variety of co-factors. Hsp70 consists of two domains: an ATPase domain (NBD) and a substrate-binding domain (SBD). Its activity is modulated by the interaction between these two domains and additionally by interactions between these domains and co-chaperones such as the Hsp40 proteins, also known as J proteins, and nucleotide exchange factors (NEFs), which facilitate ADP release and nucleotide exchange after ATP hydrolysis [4, 25, 135, 136]. The earliest NMR experiments with Hsp70 revealed a different interaction state of a model peptide with DnaK compared to GroEL, with extended versus α-helical conformation, highlighting differences in the interaction [137]. Subsequent to X-ray crystallization of the ATPase domain by the McKay lab, solution NMR techniques paved the way for the first structural characterization of the SBD of rat Hsc70 by the Zuiderweg lab [138, 139]. Subsequent work from Zuiderweg and colleagues yielded important structural and dynamical insights into Hsp90 function. Sophisticated measurements of water NOEs with the SBD of bacterial DnaK showed that several water molecules are bound to the hydrophobic binding cleft, which are displaced upon substrate binding and in this way contribute to the binding free energy of the substrate [140]. The solution structure of the DnaK SBD in complex with a substrate peptide revealed an allosteric adaptation of the molecule in agreement with earlier genetic and biochemical studies, that is in addition accompanied by a rigidification of the SBD as analyzed by ^{15}N relaxation measurements [141-144]. Based on earlier backbone assignments for the *T. Thermophilus* ATPase domain of DnaK, the analysis of the nucleotide-induced chemical shift changes, as well as dynamical changes, allowed confirmation of the proposed dynamic equilibrium model for the allosteric mechanism [145-148]. Extension of this study to a two-domain construct containing both NBD and SBD enabled for the first time analysis of the relative orientation of the two domains on the basis of chemical shifts as well as RDCs, highlighting a relatively rigid overall structure that shows allosteric adaptations due to nucleotide and/or substrate binding which are transmitted *via* subtle structural changes at the domain interface [123]. In parallel, studies on *E. coli* DnaK by the Gierasch lab revealed initially pH-driven conformational equilibria within the SBD, and showed by chemical shift perturbation and hydrogen/deuterium exchange that for the two-domain construct there is no interaction in the

nucleotide-free state and that only nucleotides drive the allosteric adaptations [149, 150]. Through combined use of RDC- and relaxation measurements it was shown that the individual domains are able to move freely on cones of about 35° with respect to each other, revealing the absence of communication between the individual domains in the absence of ATP [121], whereas the binding of ATP transduces allosteric changes along the domain interface, including subdomain rotations as part of the allosteric pathway [122]. A thorough analysis of the chemical shift changes induced by different ATP and ADP homologues of in total six different states revealed important nucleotide-induced conformational changes within the linker domain towards the SBD [151]. Extension of this study to the full-length DnaK on the basis of methyl spectra by the Gierasch lab resulted in the most detailed description of the allosteric pathway to date, highlighting the importance of the unstructured and hydrophobic interdomain linker for the allosteric transmission [88]. Screening for chemical compounds altering Hsp70 function yielded a compound that acted as co-chaperone and the preferential interaction of the anticancer agent MKT-077 with the ATP-state of bovine Hsp70 [152, 153]. Another important revelation was that different Hsp70 isoforms interact to different degrees with Tau, as analyzed by Hsp70-induced signal reduction on Tau ^{15}N-HSQC-spectra, thereby possibly explaining the different abundance of these isoforms in the brain [154].

Hsp70 function is modulated by its co-chaperone Hsp40 (DnaJ). Structure determination of the J-domain of *E. coli* DnaJ showed a three-helix bundle with a flexible tail exchanging between alternating conformations, revealing possible structural plasticity [155-157]. Additional structure determination of the homologous human J-domain of Hdj1 (Hsp40) revealed the same protein fold, thus highlighting this three-helix bundle as the general domain structure [158]. Initial analysis of the interaction of DnaK and DnaJ indicated on the basis of chemical shift perturbations that the interaction of DnaJ is modulated by the presence of ATP; this points to a binding site in close proximity of the ATP binding site on DnaK *via* the outer surface of helix II of DnaJ, which is in excellent agreement with earlier genetic studies [159, 160]. Based on interaction studies using ^{15}N-line broadening analysis of DnaK with a chimeric protein consisting of a J-domain and a DnaK client protein (p5), it was shown that the chimera showed a stronger binding affinity towards DnaK and revealed novel insight into the functional interplay of DnaJ and DnaK. In conclusion, these results suggest that the J-domain shifts the equilibrium of DnaK to a substrate-bound form, enabling more productive binding of the substrate with subsequent stimulation of the ATPase function of DnaK [161]. Subsequent determination of the solution structure of the complex of DnaK with the J-domain of DnaJ in the ADP state and in the presence of a substrate peptide confirmed the interaction *via* helix II of the J-domain with a negatively charged loop in the Hsp70 nucleotide-binding domain. Interestingly, the complex shows an unusual “tethered” binding mode which is saturable, but which has a highly dynamic

interface, in this regard comparable to the dynamic interface between the two domains of DnaK, that is not perturbed by DnaJ binding [162].

Besides DnaJ, several other co-chaperones and nucleotide exchange factors modulate DnaK, although the latter class of proteins has so far not been studied by NMR and only crystal structures of the of the nucleotide exchange factor GrpE in the free and the DnaK-bound form exist [163-165]. Mammalian Bag1 is a co-chaperone interacting with Hsc70 in an antagonistic way by suppressing refolding of substrate proteins [166]. Structure determination by solution NMR showed a bundle of three antiparallel α-helices, of which helices 2 and 3 interact with the ATPase domain of DnaK [167]. Subsequent structure determination of different members of the Bag family revealed a conserved three-helix bundle, whereas these proteins showed significant differences in the length of the respective helices and their charge distributions [168, 169].

4.3 Hsp90

Hsp90 is an evolutionarily conserved and highly abundant molecular chaperone that mediates many fundamental cellular processes including cell cycle control, cell survival, hormone signaling and response to cellular stress to maintain cellular homeostasis [170-173]. In contrast to many other chaperones, Hsp90 interacts only with a restricted number of substrate proteins (~200 in mammalians) [171, 174, 175]. Hsp90 is involved in cellular defense against cancer by directly stabilizing the tumor suppressor protein p53 among interactions with a large variety of cancer-related proteins [176]. Hsp90 is a three-domain protein, where the N-terminal domain contains the ATP binding site, the middle domain activates ATP-hydrolysis and is important for co-chaperone interaction, and the C-terminal domain is the dimerization domain [102, 177-180]. All three domains have been implicated in being involved in substrate binding, but direct data for Hsp90-C are fewer than for the other domains [181]. Hsp90 shows a high degree of structural variability, with dramatic nucleotide-dependent conformational rearrangements alternating between open and closed conformations [182, 183]. Due to the large size of the Hsp90 dimer, initial structural characterizations by NMR spectroscopy were restricted to the individual domains [102, 184, 185]. To investigate full-length Hsp90 in solution, the application of CRINEPT–TROSY [186] was needed to observe resonances to a nearly complete extent [187]. Examining the spectral properties of the core domain of the substrate p53 on the basis of [^{15}N,^{1}H]–CRINEPT–TROSY spectra revealed that it predominantly adopts an unfolded state when bound to human Hsp90 [187]. Subsequent studies by the Dyson group employed chemical shift perturbations and hydrogen/deuterium exchange to confirm that p53 core domain is in an unfolded dynamic ensemble [188]. Simultaneously, it was shown that the Hsp90 spectra only showed slight chemical shift changes giving rise to the conclusion that the interaction is highly

dynamic [189], whereas another study using yeast Hsp90 by the Kessler group showed a direct interaction *via* a hydrophilic and salt-dependent patch in the C-terminal domain with a mainly folded p53 core domain [102]. These differences in substrate binding mode may be modulated by the ionic strength, as discussed by Didenko *et al.* [190]. On the Hsp90 side, it was established that the Hsp90 dynamics are decelerated upon substrate binding [180, 181, 191]. The most accurate description of a substrate interaction with Hsp90 until now is the complex structure of Hsp90 and Tau, which revealed an extended binding interface with a multitude of binding sites to prevent aggregation of Tau [192].

Another important aspect of Hsp90 function is its interplay with a plethora of co-chaperones [178]. Chemical shift mapping revealed that the co-chaperone p23, which stabilizes Hsp90–substrate complexes [182], binds to both the N- and the M-domain of Hsp90 in a 2:2 ratio [193, 194]. This binding interface is also used by another co-chaperone, Aha1, which binds preferentially in an asymmetric way to the closed ATP-dimer, as revealed by chemical shift perturbations and biophysical analysis, leading to the closed form of Hsp90 [195, 196]. The interaction surfaces were mapped by chemical shift perturbations for further co-chaperones that bind to the N-terminal domain [197, 198] and the C-terminal domain [199]. Recently, Tah1 was identified as a new Hsp90 co-chaperone in proteomic screens, linking Hsp90 to RNA Polymerase II assembly and apoptosis within mammalian cells [171, 200, 201]. To investigate the interaction of Tah1 with the C-terminus of Hsp90, the structure of the complex was solved by solution NMR methods to medium [202] and high resolution [203]. Hsp90's role in the interaction with cancer related proteins makes it an attractive target for small molecule inhibitors, which were screened for by NMR spectroscopy [204, 205].

4.4 GroEL/GroES (Hsp60/Hsp10)

The GroEL chaperonin consists of two folding chambers, formed by heptameric rings, and a lid domain composed of the heptameric GroES, which together facilitate the folding of a substrate protein under ATP-consumption within the folding chamber [4, 28, 29, 206]. Initial experiments addressing the binding preference of GroEL for model peptides revealed a preference for α-helical peptides [137, 207], whereas subsequent analysis of a large library of synthetic peptides showed that GroEL is able to bind peptides in β-strand conformations and that the number of available hydrophobic residues is the major determinant of GroEL interaction [208]. The preference for hydrophobic residues is in excellent agreement with the interpretation of hydrogen/deuterium exchange experiments by NMR, which showed that GroEL interacts with early folding intermediates that are characteristic of non-natively exposed hydrophobic residues

[112, 113, 209, 210]. Furthermore, it was shown that GroEL activity involves multiple steps of binding and release to facilitate progression to the native fold of the substrate protein [210].

To understand the functional details of the GroEL chaperonin, the identification of the mobile segment of GroES by NMR spectroscopy was crucial, as this loop undergoes a structural transition from disorder to β-hairpin upon GroEL binding [211, 212]. Along with the observation, derived from mutational studies [213], that the apical domain of GroEL uses a hydrophobic surface to bind substrate proteins, structural studies [34, 214, 215] and NMR chemical shift perturbations [216-219] led to the identification of ATP-induced structural changes in GroEL. These changes displace the substrate from the apical domain in a positively cooperative way for all seven GroEL subunits within one ring, facilitating a complete change of the characteristics of the GroEL folding chamber from the exposure of many hydrophobic residues to the exposure of mainly polar residues [4, 220]. In a milestone NMR study on the GroEL–GroES complex, the Wüthrich group demonstrated that the combination of CRIPT (cross-correlated relaxation-induced polarization transfer) [186] and TROSY pulse schemes [221] could be used to observe backbone amide resonances within a 900 kDa protein complex [222]. [^{15}N,^{1}H]–CRIPT–TROSY spectra were observed for the GroES heptamer in complex with the GroEL tetradecamer or its single ring variant SR1-heptamer, enabling mapping of GroES-residues involved in GroEL binding on the basis of chemical shift comparison between free and GroEL-bound states [222]. Investigating the dynamics and conformational changes induced by small molecule binding to the GroEL–ES complex by ^{13}C-NMR spectra showed conformational fluctuations within the folding cage [223].

The conformations of the proteins human DHFR [224] and rhodanese [225] within the GroEL chaperonin were analyzed by 2D [^{15}N,^{1}H]-TROSY, showing resonances in the random coil region, indicating a lack of regular secondary and tertiary structure. The observed line-widths were broad, reflecting either slow tumbling of the large complex, internal motion of the bound substrate, the presence of the substrate in multiple bound conformations, or some combination of these factors. Additionally, only a fraction of the expected resonances were detected, which could suggest that parts of the chain are stably associated with the cavity wall. The dynamics of SR1-bound DHFR were also examined by comparing two different types of magnetization transfer, CRIPT and INEPT, measuring the cross-peak intensity ratio as a function of transfer time [224]. The several-fold greater signal intensity with INEPT and consistent anti-phase cross-peak character resulting from both mechanisms of transfer indicated that DHFR is not rigidly bound to SR1, but is internally mobile. Another study of rhodanese by ^{13}C-NMR confirmed that the chaperonin-bound state is largely unfolded and highly mobile [226]. An investigation of the effects on the intrinsically unstructured protein α-synuclein showed only slight changes in the

spectrum, as evidenced by a low degree of attenuation of N-terminal signals of the substrate [226]. Similar effects on the basis of ^{15}N-spectra were observed for Aβ^{1-40} and the GroEL-mediated prevention of aggregation [227]. The Clore group analyzed this interaction further by using lifetime line-broadening, dark-state exchange saturation transfer, and relaxation dispersion experiments. Global fitting of all the NMR parameters showed that the complex between GroEL and Aβ^{1-40} is transient with a lifetime of <1 ms, mediated *via* two predominantly hydrophobic segments of Aβ^{1-40}, and that the structure of the bound polypeptide remains intrinsically and dynamically disordered, with slight changes in secondary structure propensity relative to the free state [109]. A hydrogen/deuterium exchange study by NMR of human DHFR folding inside the *cis* cavity of SR1-GroEL and GroES *vs.* outside in solution observed virtually identical positions and kinetics of acquired protection during folding [111]. The recovery of native DHFR in free solution was only 50% of the input, compared to nearly 100% in the chaperonin-assisted reaction [111].

4.5 Clp Family

The Clp-family of *E. coli* belongs to the class of Hsp100-proteins and consists of unfoldases, disaggregases, and proteases, forming hexameric or heptameric ring structures [35]. The unfoldase ClpX consists of an N-terminal zinc-binding domain (ZBD) followed by an AAA+ domain [228]. X-ray crystallography yielded the structure of the ATPase domain [39], whereas solution NMR spectroscopy was used to determine the structure of the ZBD [229]. The structure of the ZBD showed a classical zinc-finger fold for the monomer [230]. Furthermore, it was shown that the ZBD exists as a dimer in solution, and a dimer-of-trimers model was thus proposed for the closed state of ClpX, which was also observed in the solution structure for *B. subtilis* ClpC [229, 231, 232]. Subsequent analysis of the binding properties of the ZBD using chemical shift perturbations showed that this domain employs mainly hydrophobic patches on its surface to recognize the substrate signal $SspB_2$, enhancing the degradation efficiency by the ClpXP unfoldase/protease machinery [233, 234]. Investigating the interaction of the ZBD with the λO replication initiator protein revealed an overlapping binding site with the ClpX co-factor $SspB_2$, highlighting the role of the ZBD in unfolding/degradation recognition [235].

Furthermore, the unfoldase ClpX forms a complex with the tetradecameric protease ClpP [73]. Investigations of the dynamical properties of ClpP by relaxation dispersion measurements showed that the interface between the heptameric rings exchanges between two distinct states, designated open and closed conformations, respectively [236]. Probing the functional relevance of this observation by locking these dynamics using cysteine crosslinks revealed that this opening between the heptameric half-rings is important for substrate release [236]. To address

the gating mechanism of the substrate entry side, specific labeling of cysteines with methyl groups showed multiple conformations, in excellent agreement with the observations of different crystal structures [73, 237, 238].

The modulation of the ClpB disaggregase by DnaK was already established biochemically [49-51], but a recent study by the Kay lab determined the structural basis of ClpB–DnaK complex formation, revealing new insights into the actual disaggregase mechanism [48]. A combination of chemical shift perturbations of methyl groups and PRE measurements led to the determination of an atomic resolution model of the ClpB–DnaK complex. Additionally, chemical shift mapping revealed that the binding side of ClpB on DnaK overlaps with the interaction surface of the nucleotide exchange factor GrpE. Taking these structural details together, a functional mechanism was proposed: i) DnaK in complex with DnaJ binds to the aggregate, and the SBD of DnaK engages the substrate. ii) DnaK binds to ClpB, followed by substrate incorporation into ClpB. iii) substrate binding to ClpB is coupled to ATP-hydrolysis, which is required for threading the substrate through the ClpB pore. iv) DnaK receives the unfolded substrate and uses its ATPase chaperone activity in collaboration with DnaJ to refold the substrate [48, 239]. Furthermore, it was shown by DOSY NMR and saturation transfer difference measurements that the yeast homologoue of ClpB, Hsp104, is able to disaggregate prion-fibrils of the yeast prion Sup35 and dissociate them *via* a hexameric intermediate into the monomeric form [94].

4.6 Proteasome

The structure of the 20S proteasomal core particle (CP) has been obtained by X-ray crystallography for a variety of organisms, revealing a conserved cylindrical structure of 28 subunits [74, 240-243]. Subsequently, NMR studies by the Kay group have made a number of notable contributions to understanding of the mechanistic details of proteasome gating and its inherent dynamics. Using the *T. acidophilum* 20S CP, consisting of different heptameric rings ($\alpha_7\beta_7\beta_7\alpha_7$) forming two antechambers ($\alpha_7\beta_7$) and a catalytic chamber ($\beta_7\beta_7$) harboring the catalytic site, enabled the use of different subassemblies, including a monomeric α-subunit, a heptameric α-ring, and a double α-ring of 14 subunits, thereby providing a clearer view for many of the processes analyzed [244]. Using selective introduction of methyl groups into the N-terminus made it possible to gain insight into the actual gating mechanism by the flexible N-termini of archaeal proteasomes, determining that on average two out of the seven chains pass through the α-annulus (the proteasome entry gate) to the proteasome interior, thereby blocking the entry passage for protein substrates, as identified by additional PRE experiments [245]. The gating mechanism is regulated by the stochastic movement between the in- and out-states on a

timescale of seconds, whereas the N-termini additionally show extensive dynamics on the ps–ns timescale [237, 245, 246]. Extending these gating studies by the usage of magnetization exchange measurements to higher viscogens and even cell lysates showed similar dynamics for the motions of the N-terminus, indicating only a limited effect from molecular crowding within the cellular compartments [247]. The proteasomal CP needs to be activated by the 11S activators that bind to both exposed sides of the α_7-rings of the CP, inducing allosteric changes within the catalytic chamber as evidenced by methyl-group chemical shift perturbations about 75 Å away from the 11S binding site, and resulting in an alteration of the relative populations of interchanging CP conformers [248]. This distinct allosteric regulation was further shown within HslV, that together with its unfoldase HslU forms a simplified bacterial "proteasome", indicating that the dynamics as well as the plasticity in HslV and the proteasome are critical aspects for the function of these barrel-like proteases [249]. It was also demonstrated that the interior surface of the proteasome stabilizes an unstructured conformation of translocated substrates, thereby preventing refolding of stable protein domains inside the proteasome [250]. In addition, methyl-TROSY based experiments have guided new approaches to developing proteasome inhibitors by demonstrating that inhibition can be achieved by binding in the vicinity of the interface between α and β subunits in a manner independent of binding to the active sites [251]. Overall, these remarkable achievements were made possible by the combination of selective labeling of methyl groups of amino acids in a deuterated background and the development of methyl-TROSY [6]. Furthermore, it was shown that binding of a small molecule inhibitor of proteolysis alters the distribution of the different CP conformers [248], which led to the design of a new fluorine-containing substrate to be able to follow the allosteric changes induced by small inhibitors by ^{19}F-NMR [252]. Studies of the actual proteolysis mechanism by threonine-methyl spectra indicated that Thr1 acts as a base in the first step of peptide-bond cleavage [253]. Furthermore, as a proof of principle, sequential backbone assignment of the α-subunit within the 1 MDa full proteasome (11S-$\alpha_7\beta_7\beta_7\alpha_7$-11S) was shown to be feasible by magic angle spinning (MAS) solid-state NMR spectroscopy [115].

4.7 SecA

To translocate polypeptides *via* the SecYEG-translocon across the bacterial inner membrane towards the periplasmic space, the substrate has to be delivered by the SecA chaperone [254, 255]. Besides its molecular chaperone function, SecA serves as the initial recognition site for the signal sequence and as the motor domain of the SecYEG-channel, whereupon it uses the energy generated by ATP-hydrolysis [256]. Substrate proteins are delivered by the cytoplasmic chaperone SecB to SecA. Initially it was shown by hydrogen/deuterium experiments that SecB

interacts with unfolded polypeptides [209]. SecB contains a highly flexible C-terminus [257] and possibly interacts through this region with the extreme C-terminus of SecA, which forms a zinc-finger motif as shown by early solution structures [258, 259]. SecA consists structurally of a discontinuous helicase motor domain (formed by the ATP-binding domain), the intramolecular regulator of ATP hydrolysis (IRA), the preprotein-binding domain (PBD), and the C-terminal domain, which is involved in protein dimerization [256, 260, 261]. Initially, two distinct flexible regions were identified based on 2D [^{15}N,^{1}H]-HSQC spectra, which are involved in Mg^{2+}-binding and undergo conformational changes within the SecA cycle [262]; these changes could subsequently be attributed to an order–disorder equilibrium that the SecA motor uses for its function [263]. ATP-hydrolysis occurs at a site sandwiched between the helicase motor sub-domains, inducing these conformational changes within the motor domain [261, 263, 264].

Early transferNOE (trNOE) and line-broadening studies to determine the structure and important binding residues of signal peptide interaction made use of a solubility-enhanced variant of the outer membrane protein LamB signal peptide bound to SecA [265]. The observed trNOEs showed that the bound signal peptide adopts an α-helical structure and differential line broadening results suggested that the initial signal sequence-binding pocket on SecA diplays both electrostatic and hydrophobic character [265]. Subsequently, the PBD was identified by NMR chemical shift perturbations and selective photoaffinity measurements as the site where preproteins bind on SecA [254, 260, 266] and it was shown that this domain is able to control conformation and ATP catalysis within the helicase motor [267]. The most accurate structural information to date was reported by the Kalodimos group, obtained from high-resolution NMR structure determination in combination with PRE measurements of a LamB signal sequence bound to the SecA protein [260]. It was shown by temperature-induced chemical shift perturbations that the PBD region is highly flexible, as evidenced by extensive intrinsic temperature-dependent conformational changes. These changes are modulated by the C-terminal domain [267], which in turn is the dimerization domain of the SecA protein [262]. While it still remains debatable whether the active SecA functions in the dimeric or monomeric state, it was shown by measuring the folding kinetics with fluorescence and CD-spectroscopy that SecA folds *via* a dimeric intermediate, and exists in an equilibrium between monomer and dimer in the cellular environment [268]. In addition, the lack of functional details of the complete SecYEG-machinery is reflected by the fact that only one pilot study by NMR spectroscopy has so far been reported on this system: by using dynamic nuclear polarization (DNP) enhanced solid-state NMR spectroscopy, an α-helical conformation of the LamB signal peptide within the SecYEG-translocon was shown [269].

4.8 Skp and other periplasmic chaperones

After translocation into the periplasm of *E. coli* and other Gram-negative bacteria, outer membrane proteins bind to the most abundant chaperones Skp (seventeen kilodalton protein) and SurA (survival factor A) [270, 271]. SurA is structurally related to trigger factor and might bind substrates in a dimeric or monomeric fashion, as observed by X-ray crystallography for different model peptides [272, 273]. In contrast, Skp forms a trimer with long protruding coiled-coil helices encompassing the outer membrane protein binding chamber [274, 275], which binds its substrates in a 1:1 fashion of trimer to monomer [276]. Initial NMR experiments with two-domain OmpA bound to Skp showed domain discrimination of the chaperone for the β-barrel domain [277]. On the basis of secondary chemical shifts it was shown that adjacent parts of the coiled coils of the Skp tentacles undergo different adaptations. Whereas the main parts are rigidified upon substrate interaction, a pivot element remains flexible, possibly as a structural buffer against fluctuations of the substrate conformation [84]. NMR relaxation data confirmed these observations, as the amplitudes of motions on the ps–ns timescale were generally reduced for most parts of the protein, but the pivot element retained its inherent mobility. Intermolecular PRE data were used to determine the compactness of the bound substrate ensemble, while extensive intermolecular PRE measurements allowed structural placement of the Omp protein in the Skp cavity [84]. Preliminary experimental observations indicate that the chaperone-bound state of Omps bound to SurA exhibits a similar conformational averaging [84, 278].

Structure determination of FkpA, another periplasmic chaperone, revealed an extended V-shaped dimeric protein with the dimerized chaperone domain linked *via* a long α-helix to a PPD [279, 280], in excellent agreement with earlier crystallographic studies [281]. Relaxation studies demonstrated the conformational flexibility between the chaperone domain and the PPD, which was further supported by RDCs, which indicate the absence of a fixed orientation between the two domains due to the structural plasticity of the linker α-helix [280]. Upon substrate binding, the flexibility of the linker helix is reduced and chemical shift mapping of the interaction surface revealed shielding of the substrate from the aqueous environment by burying it deeply [280].

PpiD is anchored *via* an N-terminal membrane helix to the inner membrane and its three soluble domains face the periplasmic space [282]. Structural and biochemical analysis of the parvulin-fold PPD of PpiD showed that it closely resembles the parvulin domain 1 of SurA, which itself is in the core of the SurA substrate binding site, indicating that within PpiD the parvulin domain might have a similar function [283].

4.9 αB-crystallin

αB-crystallin (αB, 20 kDa) belongs to the family of small heat shock proteins (sHsp) that help to maintain protein homeostasis by interacting with unfolded, aggregated or misfolded proteins to prevent cell damage [2, 284, 285]. This class of chaperones works in an ATP-independent manner [286]. αB was originally identified as the B-subunit of α-crystallin, a protein essential for maintaining eye-lens transparency. In recent years, the list of biological roles for αB has grown substantially, including involvement in the regulation of the ubiquitin-proteasome pathway as well as apoptosis, and dysfunctions of αB in humans are associated with the occurrence of many neurodegenerative diseases such as Alzheimer's disease [287-292]. A common feature of αB-crystallin and most sHsps in general is the formation of polydisperse, supramolecular complexes with a variable number of subunits (~24–32), whose inherent dynamics are an important feature and prerequisite for function [293]. This polydispersity and dynamics have prevented structure determination by crystallography. Initial investigations by solution NMR spectroscopy of related sHsps revealed that the C-termini of αB-crystallin, mouse Hsp25, and rat Hsp20, as well as the C-terminus of βA-crystallin, are highly flexible and devoid of secondary structure, as evidenced by nearly random coil Cα chemical shifts, and are not involved in oligomerization [294-297]. Subsequent analysis demonstrated that these flexible extensions are not directly involved in substrate binding, but play an important role in retaining the quaternary structure, as evidenced by increased flexibility observed by ^{1}H-spectroscopy upon C-terminal truncation of mouse Hsp25, and subsequently by altered chaperone activity upon C-terminal immobilization of αA-crystallin through the introduction of bulky amino-acids [298, 299]. Investigation of the dynamics of the C-terminus of αB-crystallin showed the importance of this region for the solubility of αB-crystallin complexes [300]. Saturation transfer difference (STD) experiments showed that αB-crystallin interacts with the hydrophobic core of $A\beta^{1-40}$ [301]. Furthermore, the ability of αB-crystallin to prevent oligomerization and the oxidation of Met35 was established, whereas the oxidation of Met35 in $A\beta^{1-40}$ induces an increased neurotoxicity, since the oxidized form facilitates the propagation of free radicals among adjacent residues [301-303]. Based on combined NMR, PRE and relaxation experiments, as well as mass spectroscopy, a comprehensive picture of αB-crystallin emerges in which quaternary dynamics and oligomeric distribution due to monomer exchange on a timescale of minutes are connected to structural fluctuations in the C-terminus on the millisecond timescale [304, 305].

A first structural characterization of αB-crystallin using a hybrid approach of solution and solid-state NMR revealed that the general topology in the isolated as well as the oligomeric forms with six β-strands remains the same, and only secondary chemical shift changes could be observed at the presumed interaction surfaces [306]. Subsequent structure determination by solid state

NMR showed that the αB-crystallin core domain lacking its flexible termini forms a curved dimer with the secondary structure elements identified earlier. This curved dimer serves as a building block for the oligomeric assembly containing twelve of these dimers assembling to 24-subunit oligomer of αB-crystallin with tetrahydral symmetry, as shown by SAXS measurements [118]. Although this proposed oligomer of 24 subunits is consistent with earlier cryo-EM studies, it populates only about 5 % of the existing multimers, as shown by mass spectroscopy [293, 307]. Solid-state NMR measurements demonstrated that the polydispersity is governed by the high flexibility of the αB-crystallin termini. The N-terminus can form two β-strands in a diversity of environments, which thus can contribute to higher order oligomers, in which additional dimers fill existing openings in the 24-mer, as additionally shown by EM and SAXS measurements [308, 309]. Furthermore, a relaxation study in both solution and the solid state established that at least two distinct structural environments are adopted by the C-terminal IxI residues of αB-crystallin, one free and one bound, with relative populations varying substantially with temperature [310, 311]. To explore the role of copper in the assembly and function of αB-crystallin, a combined solid-state/solution NMR approach was chosen that revealed a copper interaction site with picomolar affinity at the dimer interfaces, as well as structural reorganization of the N-terminus, leading to an increased heterogeneity of the αB-crystallin-oligomers [116]. Characterization of the interaction of αB-crystallin with substrates initially showed that the chaperone interacts preferentially with exposed hydrophobic regions as observed in the ^{1}H spectra of the aromatic region of α-lactalbumin [312]. Subsequent analysis of the interaction with β_2-microglobulin showed that αB-crystallin interacts in a non-specific manner to prevent unfolding, nonfibrillar aggregation and fibril formation [313]. This preference for hydrophobic and exposed residues was recently confirmed with interaction studies of αB-crystallin with a cataract-related γS-crystallin variant using chemical shift changes [314].

4.10 BamA

BamA is an insertase from the Omp85 family of proteins. It forms the central unit of the Bam complex, which is responsible for the insertion of membrane proteins into the outer membrane of *E. coli* and other Gram-negative bacteria [315, 316]. The long loop L6 of BamA shields the barrel pore from the outside and may play an important role in BamA function [68]. A recent solution NMR study in several membrane-mimicking environments showed that this loop is highly flexible compared to the rest of the protein [317], in excellent agreement with data from solid-state NMR [318, 319]. Further NMR studies were directed to investigate the structural and dynamic properties of the periplasmic POTRA domains (polypeptide transport associated

domains). The solution structure of a two-domain construct of BamA-POTRA domains showed no indication of dimerization [320], indicating that the observed crystal contacts correspond to non-native β-augmentation [321-323]. Additionally, experiments addressing substrate binding by POTRAs *via* β-augmentation were reported [320]. It was shown by solid-state NMR that the soluble POTRA domains and the membrane-embedded part of BamA show significant differences in their respective mobilities [324] within precipitated samples, but that these POTRA-movements are significantly restricted when the protein is reconstituted in proteoliposomes [319]. Contributions by NMR on other translocases and insertases have so far remained sparse and the interested reader is referred to excellent recent reviews [23, 59, 325, 326].

4.11 Other chaperones

Prefoldin is a heterohexameric ($\alpha_2\beta_4$) archaeal and eukaryotic cytosolic chaperone of ~90 kDa size, exhibiting a "jellyfish" structure with six α-helical coiled-coil arms, with similarities to the periplasmic chaperone Skp discussed above [274, 275, 327]. At the tips of the prefoldin arms, the coiled coils are partially unwound to expose hydrophobic residues for interaction with non-native proteins [328]. Functionally, it was shown that prefoldin is able to bind, release, and transfer its substrate towards a chaperonin in an energy-independent manner [327, 329]. To study how the dynamics of prefoldin are affected by the interaction with the chaperonin, it was amino-acid type selectively labeled with [1-^{13}C]-methionine and the corresponding carbonyl resonances analyzed [330]. The methionine residues cluster in the tip region of prefoldin and these residues show a high degree of flexibility in the apo-state, which only vanished for Met11 of the β-subunits, indicating a direct interaction on binding to the chaperonin [330]. The retention of flexibility in the methionine resonances within prefoldin is accompanied by a similar behavior of methionine residues in the C-terminal region of the chaperonin, and might be an important feature for the chaperone activity of the complex as a similar effect has already been reported for GroEL to enhance the folding speed within the cavity [330, 331]. Recently, a pioneering study on an eukaryotic HSP60 protein, the group II chaperonin TRiC (TCP-1 ring complex) revealed that intrinsic flexibility of the substrate-binding site allows substrates to bind in a multitude of conformations to the same apical domain and that the unique substrate-binding motifs in the different TRiC subunits enable a variety of substrates without sequence similarly to bind [332].

PrsA, a trigger factor/SurA-like protein from Gram-positive bacteria, is a 30 kDa lipoprotein localized in the space between plasma membrane and cell wall and involved in the biogenesis of secreted proteins [333, 334]. Structural characterization by solution NMR of the PrsA PPD

domains of *S. aureus* and *B. subtillis* revealed a typical parvullin fold for these domains [335, 336]. The fold showed highly similar structures reported for trigger factor and SurA PPD domains from Gram-negative bacteria [130, 272]. Mapping the binding site of a substrate peptide by chemical shift perturbations revealed a highly negatively charged pocket of PrsA PPD [336]. Extending the structural studies to full-length PrsA revealed a dimeric structure by X-ray crystallography, that could be confirmed by solution NMR experiments [337].

Tim chaperones are hetero hexameric proteins consisting either of Tim8–Tim13 or Tim9–Tim10 complexes forming a barrel-like shape with protruding α-helices, that reside within the inner-membrane space of mitochondria and resemble functionally and structurally the periplasmic Skp [274, 275, 338, 339]. ^{15}N-HSQC spectra showed that the individual subunits are largely unfolded in their reduced assembly-incompetent state and revealed a molten globule state in their oxidized assembly-competent state [340].

Hsp33 is another redox-regulated chaperone, which exists under the reducing conditions of the bacterial cytosol in an inactive monomeric form, but which becomes activated upon oxidative stress to function as a potent molecular chaperone [341, 342]. Careful investigation revealed a two-step activation involving three distinct states: in the inactive-state the C-terminus exhibits a stable fold that masks the substrate-binding site. Four cysteines stabilize this interaction by coordinating a Zn^{2+}–ion. Upon oxidative stress the cysteines form disulfides and detach from the substrate-binding site, and the secondary structure within the C-terminus is lost, leading to a partly active monomer. These partly active monomers quickly associate together to give the fully active Hsp33 dimer, forming a swapped dimer with an extended substrate-binding site [343-345]. Subsequent analysis of the structure of the C-terminal in the Zn^{2+}–state revealed a unique fold of three α-helices surrounding two β-strands [346].

Hsp47 is a specific chaperone for collagen in the endoplasmic reticulum of eukaryotes, preventing unfavorable aggregation in the early secretory pathway of collagen [347, 348]. By specifically labeling the tryptophan ε-indole resonances and backbone amide resonances of histidines, the binding site of the collagen could be mapped, indicating that binding induced large conformational changes within Hsp47 [349].

5 Adaptations of chaperones to their substrates

This section reviews the contributions of NMR spectroscopy towards characterizing the adaptation mechanisms of chaperones to their substrates. Two main forms of adaptation can be distinguished, namely changes in chaperone structure and changes in chaperone dynamics.

5.1 Structural adaptations

Since the first description of allostery by Monod *et al.* [350], it has become evident that nature uses this form of regulation widely for enzymes and molecular machines to carry out their respective biological functions. Many chaperones also use ATP-dependent allosteric changes as part of their functional cycles. One of the most intensively studied allosteric chaperone mechanisms is the intricate regulation of DnaK (recently reviewed in [136]). Extensive work of the Zuiderweg and Gierasch labs showed that this allosteric mechanism comprises three distinct protein conformations [88]. These conformations differ in the relative arrangements of the three domains of DnaK, the NBD, the SBD, and the lid domains, whereas the interdomain linker and a flexible helix embedded in the lid domain provide the allosteric coupling connection. This arrangement provides Hsp70 with properties to transfer allosteric signals between its domains as a result of nucleotide and/or substrate binding [351-353]. The origin of the allosteric signaling lies in the NBD, which upon ATP binding experiences intradomain conformational changes leading to a higher affinity for the interdomain linker [122, 146, 151]. Furthermore, binding of the substrate is directly coupled to these NBD conformational changes due to its direct stabilizing effect on the SBD lid interface and an indirect destabilizing effect on the NBD–SBD interface, clearly showing that each of these two endstates comprises distinct intrinsic interactions between two structural elements simultaneously, whereas the third state is a transition state showing interactions between all three structural elements [88]. The identification of this intricate allosteric network by NMR explained earlier observations that mutations within the SBD–lid interface led to a decrease in substrate affinity and that ATPase stimulation is coupled to substrate affinity [354-356].

Despite the fact that available high-resolution crystal structures of the proteasome core particle showed only the existence of a single conformation [75], NMR chemical shift perturbations revealed the existence of an allosteric network underlying the proteolytic function [248]. These allosteric effects are induced by binding of the 11S-activator leading to structural changes 80 Å away from the interaction site [248]. This allosterically coupled proteolysis is shared by the bacterial HslU–HslV system, as revealed by X-ray studies [72]. Binding of HslU to the HslV-protease leads to a shift of the apical helices, leading to conformational changes propagating towards residues proximal to the active site and leading to an increased proteolysis rate [357]. By combined analysis of a mutational study, chemical shift perturbations and relaxation dispersion experiments using methyl TROSY it was found that HslV is an inherently plastic molecule. Upon HslU interaction it undergoes concerted millisecond timescale dynamic processes that couple substrate binding and proteolysis to HslU binding [249].

5.2 Dynamic adaptations

Besides structural reorientations, changes in protein dynamics remain a mechanistic possibility for chaperones to bind substrates. A detailed study of the dynamic adaptions of a chaperone upon substrate binding was performed by Burmann *et al* for the Skp–Omp complexes [84]. 2D [^{15}N,^{1}H]-correlation spectra showed only slight chemical shift changes between apo and holo forms. Importantly, the observation of a single, coherent set of NMR resonances for both the apo and the holo forms shows that each of the three Skp protomers samples the same conformational space, despite binding an asymmetric substrate [84]. Extensive measurements of ^{15}N relaxation parameters showed a general reduction of the fast backbone motions on the ps–ns timescale upon substrate binding. On the other hand, the overall molecular tumbling of the Skp chaperone is not substantially affected by binding of the substrate, which is further shown by the already mentioned absence of substantial chemical shift changes and highly similar SAXS curves for the apo and holo-states of Skp (our unpublished data). The observed flexibility might represent a general feature of molecular chaperones, enabling them to bind to a broad range of substrates. After initial interaction the chaperones might in general reduce their flexibility, to stabilize the chaperone–substrate interaction.

Comparable results were obtained by Saio *et al.* for the interaction of trigger factor and PhoA [91]. Upon addition of PhoA or different PhoA sub-constructs the authors observed only slight chemical shift perturbations of the chaperone, leading to highly similar NMR structures in the presence of three different PhoA sub-constructs, showing an all-atom rmsd between them of 1.5–2.2 Å. Comparing these three NMR structures to the previously determined high-resolution X-ray structure (1W26; [19]) indicates only slight rearrangements of the individual domains towards each other, as evidenced by an only slightly increased all-atom rmsd of 2.3–3.4 Å. Furthermore, an increased rigidity within the SBD, which features the main substrate binding sites, was also observed upon substrate binding.

During the determination of the solution structure of the SBD of DnaK, Pellecchia *et al.* observed extensive line-broadening for a part of β-strand 3, that seems to not be formed in solution in contrast to earlier crystal structures [144, 358, 359]. Initial titration measurements with different DnaK binding peptides showed [^{15}N,^{1}H]-correlation spectra devoid of the previously observed excess of line broadening for the apo state [144]. Subsequent determination of the solution structure of the DnaK-SBD in complex with an eight-residue polypeptide showed distinct, widespread, and contiguous differences in structure extending toward areas previously defined as important to the allosteric regulation of the Hsp70 chaperones [141]. ^{15}N NMR relaxation data indicated that the SBD in complex with the peptide is a relatively rigid molecule leading to a shift in monomer–dimer equilibrium as NMR diffusion measurements revealed that

the dimeric apo-SBD monomerizes upon substrate peptide binding [141]. Detailed analysis of these relaxation data revealed only low mobility on the ps–ns timescale and the absence of conformational exchange on the millisecond timescale [141, 360].

6 Chaperone–substrate complexes characterized by NMR spectroscopy

While numerous studies of chaperones in their apo forms and as part of chaperone–substrate complexes have been published, detailed descriptions of the substrates as part of chaperone–substrate complexes have remained difficult challenges. This section summarizes studies in which the conformational states of substrates were characterized by NMR spectroscopy, and then reviews in more detail three examples in which a description of the substrate was established at atomic resolution.

Park *et al.* investigated the complex between Hsp90 and the core domain of its substrate p53 [188, 189], with the intriguing finding that p53 binds Hsp90 in a molten globule-like state [188]. Subsequent investigations of the p53 dynamics within Hsp90 revealed that such a dynamic interaction may be modulated by co-chaperones, but the dynamic and non-specific nature of the interaction in the absence of these factors may also provide an explanation for the observed wide range of structure and sequence types in the client proteins of Hsp90 [189]. A relatively nonspecific interaction, with multiple possible binding sites throughout the molecule, might lend itself at the same time to a wide client specificity and a low enough affinity that the client can readily dissociate from the chaperone under the right circumstances [189].

Based on the analysis of multiple NMR parameters, the Clore group showed that the complex between GroEL and $A\beta^{1-40}$ is transiently formed with a local lifetime of <1 ms and that the structure of the bound polypeptide remains intrinsically and dynamically disordered, with minimal changes in secondary structure propensity relative to the free state, as an intrinsically unstructured protein [109]. This recent observation for GroEL is in excellent agreement with earlier observations showing that GroEL does not recognize the classical molten globule state of a model substrate, R-lactalbumin (RLA) [361], but that it binds less organized forms of the same state [362, 363].

To investigate the states of substrate proteins within the proteasome, the Kay group linked the substrates covalently to the antechamber [250]. Analysis of the chemical shifts showed that the substrates are held in an unfolded, highly dynamic state within the proteasome. Intermolecular PRE experiments confirmed that the tethered substrate proteins are located exclusively within the antechamber cavity. Furthermore, these results showed a uniform effect on the analyzed

methyl groups, leading to the conclusion that substrate residues lack unique, position-dependent direct interactions with the cavity surface, suggesting that the substrate state is best described as an ensemble of dynamic, interconverting, unstructured conformations [250].

6.1 Trigger factor–PhoA: The 'beads on a string' arrangement

The bacterial chaperone trigger factor binds selected segments of its substrate PhoA in unique conformations. In a seminal work, the Kalodimos group recently determined the high-resolution structures of these complexes [91]. By using a divide-and-conquer approach for initially mapping and subsequently determining the structures of the interaction sites, four distinct peptide-binding sites on trigger factor were revealed that are situated in the SBD as well as the PPD, extending over a distance of 90 Å. As it is generally assumed that chaperones mainly interact with exposed hydrophobic segments of substrate proteins to prevent aggregation [1], the sequence-dependence of the PhoA hydrophobicity was analyzed [91], revealing that it is the most hydrophobic segments that are bound to trigger factor. A thorough isothermal titration calorimetry (ITC) analysis of different PhoA peptides led to the identification of seven different sites of PhoA that are able to form stable complexes with trigger factor. On the basis of this segmental approach, and additionally supported by MALS (Multi angle light scattering) data, the authors showed that three trigger factor molecules bind a single PhoA molecule [91]. The binding affinity gradually increased with the length of the engaging PhoA-sub-construct until all four binding sites in trigger factor were fully occupied [91]. This observation exactly describes the situation in the context of the translating ribosome, where trigger factor engages with nascent polypeptides after the first ~100 amino acids are synthesized [19, 20, 124].

Split into three parts, individual PhoA segments form 1:1 complexes. The use of selective labeling of the methyl groups of alanine, methionine, threonine, isoleucine, leucine, and valine as well as specific labeling of the aromatic residues tryptophan, tyrosine, and phenylalanine made NOE-based structure determination of these ~60 kDa complexes possible. On the basis of 1200–2000 intramolecular and 60–80 intermolecular NOEs, the structures of trigger factor and three different complexes with PhoA constructs were calculated (Figure 3). All of these high-resolution structures showed an extended binding interface on the trigger factor surface, whereas PhoA is bound in an extended conformation. The dissociation constants of the individual complexes are in the range from 2 to 14 μM. The binding arrangement depicted in Figure 3a represents the lowest energy state for the sub-construct – this conformation is populated to at least 70% [91]. Based on relaxation dispersion measurements, the local lifetime of the individual PhoA-sub-constructs to trigger factor was determined as ~20 ms. Interactions similar to the 'beads on a string' model described here were also reported between the

periplasmic chaperone SurA and different Omp-derived peptides by X-ray crystallography, and for the SecB-chaperone on the basis of EPR measurements [273, 364]. Furthermore, a similar extended binding mode for DnaK was recently reported by single-molecule spectroscopy by the Schuler lab [42].

6.2 Hsp90–Tau: An extended ensemble

Using a combination of NMR and SAXS, Karagöz *et al.* derived a structural model of Hsp90 in complex with its natural disease-associated substrate, the intrinsically disordered Tau protein [192]. On the basis of signal intensities in 2D [^{15}N,^{1}H]-correlation spectra of Tau in the absence and presence of Hsp90, a direct binding interaction on the intermediate exchange time scale was shown, in agreement with the affinity determined by fluorescence spectroscopy. The Hsp90-interacting Tau segment shows a net positive charge and a considerably higher content of hydrophobic residues compared to the non-interacting parts of the protein [192]. To map the interaction surface on Hsp90, the authors used selectively isoleucine-labeled Hsp90, revealing chemical shift changes and splittings of isoleucine methyl resonances on both the N- and M-domains of Hsp90. Thereby, individual interaction sites were up to ~100 Å apart revealing an extended interaction surface of about 840 Å^2. Furthermore, addition of ATP to the Hsp90–Tau complex increased the dynamics of the chaperone, as evidenced by dramatically sharpened lines for a subset of isoleucine methyl resonances, marking a possible important aspect of Hsp90 function [192]. To complement this local arrangement of Hsp90 and Tau, the authors employed SAXS measurements to obtain the overall shape of the complex in solution. They observed an extended state for the Hsp90 dimer in solution, in agreement with earlier SAXS studies for different Hsp90 homologues [192, 365, 366]. SAXS measurements of the Hsp90–Tau complex revealed no modulation of the Hsp90 shape. Subsequent combination of the NMR and SAXS data led to a structural model in which the N-terminal domains are the most distant points of the dimeric structure (Figure 4A). The segments of the Tau ensemble in close proximity to Hsp90 are strongly converging on their respective binding site, exhibiting minimal widths of 19 Å and 17 Å at the most narrow sites on Hsp90-N and Hsp90-M, respectively. In contrast, the disordered segments of Tau that are not bound to Hsp90 show a high degree of conformational heterogeneity (Figure 4B). The identification of this rather broad interaction surface and significant flexibility of Tau bound to Hsp90 is indicative of reorientation of the chaperone as part of the substrate binding. This observation is further underscored by the mechanistic aspect that this large binding region allows for a high number of low-affinity contacts to build up overall high-affinity binding despite the absence of a binding pocket or cleft [192].

6.3 Skp–Omp: The fluid globule state

To obtain high resolution information about the state of an outer membrane protein (Omp) bound to the periplasmic chaperone Skp, a combination of relaxation measurements, line-broadening analysis, PRE measurements, and subsequent analysis of intermolecular methyl–methyl NOEs was used [84, 85]. Analysis of the [^{15}N,^{1}H]-correlation spectra of the native substrates OmpX and tOmpA (transmembrane domain of OmpA) featured a complete set of resonances showing only small dispersion of ~1 ppm in the proton dimension, indicating fast conformational averaging of an ensemble of unstructured conformations. This lack of secondary structure elements was further evidenced by the combined secondary chemical shifts, which mainly resemble random-coil chemical shifts [84]. The absence of chemical shift differences with the random-coil state is evidence that the Omp polypeptides undergo fast conformational averaging over multiple backbone conformations with individual lifetimes of each conformation of < 1 ms. Detailed relaxation analysis of this chaperone-bound state revealed a large amplitude of motions on the ps–ns timescale. Concomitant analysis of the dynamics of the Skp revealed a dynamical decoupling of chaperone and substrate, as only the slow motions of the Omp showed an increase in comparison to the random-coil state in chaotropic denaturant guanidinum/HCl [84, 367].

Intermolecular PRE measurements were used to address the degree of compactness that the Omp protein features in the Skp cavity. The observation of a global, average relaxation enhancement effect for the whole Omp polypeptide enabled first order approximation model calculations of the constrained polypeptide yielding a spherical volume with a radius of 21 Å. Use of intermolecular PREs permitted the placement of the Omp within Skp, and this model was extensively cross-validated by a four different sets of PRE measurements. In addition, earlier chemical cross-linking data [277] and small angle X-ray scattering data (our unpublished data) confirmed binding of the Omp within the cavity of Skp. To complete the biophysical description of the Skp–Omp complexes, their global lifetime was determined by time-dependent PRE exchange experiments on the basis of ^{15}N-^{1}H correlations, yielding a global lifetime of 2.6 hours for the Skp–OmpX complex. The difference of seven orders of magnitude between the global and local lifetimes reveals the avidity effect as the underlying mechanism for the high-affinity interaction between chaperone and substrate. In the case of Skp, a multitude of weak interactions combine to give the high global binding affinity, resulting in a dissociation constant in the low nanomolar range, as observed for typical Skp substrates [276]. As this PRE-derived structural model yielded only long-range spatial correlations between the chaperone and its substrates, subsequently the possibility of using methyl–methyl NOEs to detect specific short-range contacts was examined [85]. Using an orthogonal labeling approach, suitable

combinations of specifically methyl-labeled isoleucine, leucine, valine, alanine, and methionine residues were introduced into the two components. It was then possible to analyze specific intermolecular NOEs in an unambiguous manner, since they occurred in unique, non-overlapped portions of the spectra. 2D [^{13}C,^{1}H]-correlation spectra of ILV-labeled tOmpA within Skp showed that the methyl moieties tOmpA feature narrow chemical shift dispersions, closely resembling the random-coil spectrum and thus indicating that the tOmpA side chains in Skp lack a well-defined structure. The observation of a single set of resonances confirms the presence of a conformational ensemble in the fast exchange regime, that is, with individual lifetimes below 1 ms, validating the use of an ensemble model as the basis of the data interpretation and in agreement with the data for the ^{15}N-^{1}H-correlation spectra [84, 85]. Intermolecular cross-peak amplitudes measured by 3D ^{13}C-resolved [^{1}H-^{1}H]–NOESY experiments between ILV-tOmpA and A-Skp revealed intermolecular NOEs between the tOmpA and A34, A75, A78, and A86, all of which have their side-chains pointing into the central part the Skp cavity [85]. These alanine residues thus are part of the contact surface within the central part of the Skp cavity, in agreement with the previous PRE-based mapping (Figure 5) [84]. Importantly, the intermolecular NOEs are negative, indicating that the chaperone–substrate contacts are in the slow motion limit [92, 368]. This results in a lower limit of ~1 ns for the local lifetimes of segments of the substrate bound to the chaperone. Since the intermolecular NOE peaks are a superposition of individual signals from up to 45 spin probes within tOmpA, conformations with a given Skp–tOmpA ^{1}H–^{1}H spin-pair in close contact are populated to about 0.5–2% [85]. The revelation of the superposition and subsequent population of only a few percent of a given spin pair shows that in the context of a flexible protein bound to a stable protein, the analysis of NOEs as distance restraints is not warranted.

7 Conclusion and Outlook

For studies of chaperone–substrate complexes, solution NMR spectroscopy is the method of choice to capture all aspects of these typically highly dynamic interactions at atomic resolution. With recent technical developments, large protein–substrate complexes of molecular weight 100 kDa and above have now come within reach for such studies. We expect major additional contributions towards understanding the molecular basis for chaperone functions at the atomic level from NMR experiments in the coming years.

Acknowledgements

We thank Stefan Rüdiger for critical reading of the manuscript. This work was supported by grants from the Swiss National Science Foundation (Grant PP00P3_128419) and the European Research Council (FP7 contract MOMP 281764) to S.H.

Figure legends

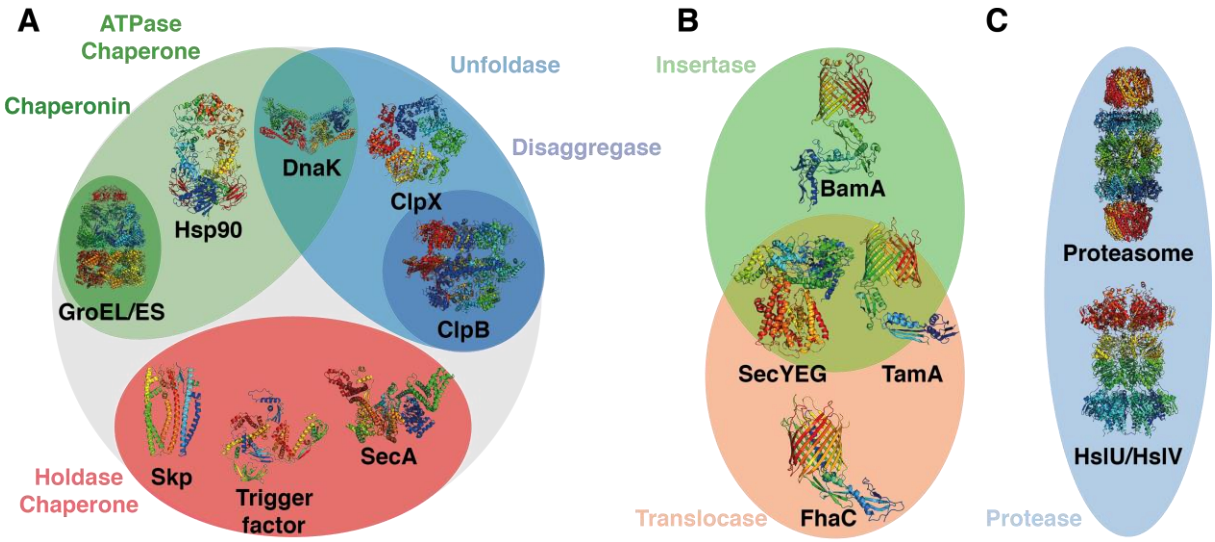

Fig. 1: Functional classes of molecular chaperones, illustrated with selected examples. **A)** Types of soluble chaperones: Chaperones with holdase function bind substrates and prevent them from aggregation [19, 275, 369]. ATPase chaperones participate in the substrate folding process and possess ATPase activity [182]. Chaperonins facilitate substrate folding within a folding chamber [34]. Unfoldases bind to misfolded proteins and unfold them. [39] Disaggregases solubilize existing protein aggregates [370]. Some chaperones exhibit overlapping functions [371]. **B)** Types of membrane-integral chaperones: Translocases transport substrates across a membrane [61], insertases fold their substrates into the membranes [64, 67, 372]. **C)** Selected protease machineries, the archaeal proteasome [75] and the bacterial HslU/HslV complex [72]. PDB IDs: Skp, 1SG2 [275]; trigger factor, 1W26 [19]; SecA, 2FSF [369]; Hsp90, 2CG9 [182]; GroEL/ES, 1AON [34]; ClpX, 3HWS [39]; ClpB, 4D2U [370]; DnaK, 4B9Q [371]; FhaC, 2QDZ [61]; BamA, 4K3B [64]; SecYEG, 3DIN [372]; TamA, 4C00 [67]; proteasome, 1YAR [75]; HslU/HslV, 1G3I [72]. See text and Table 1 for details.

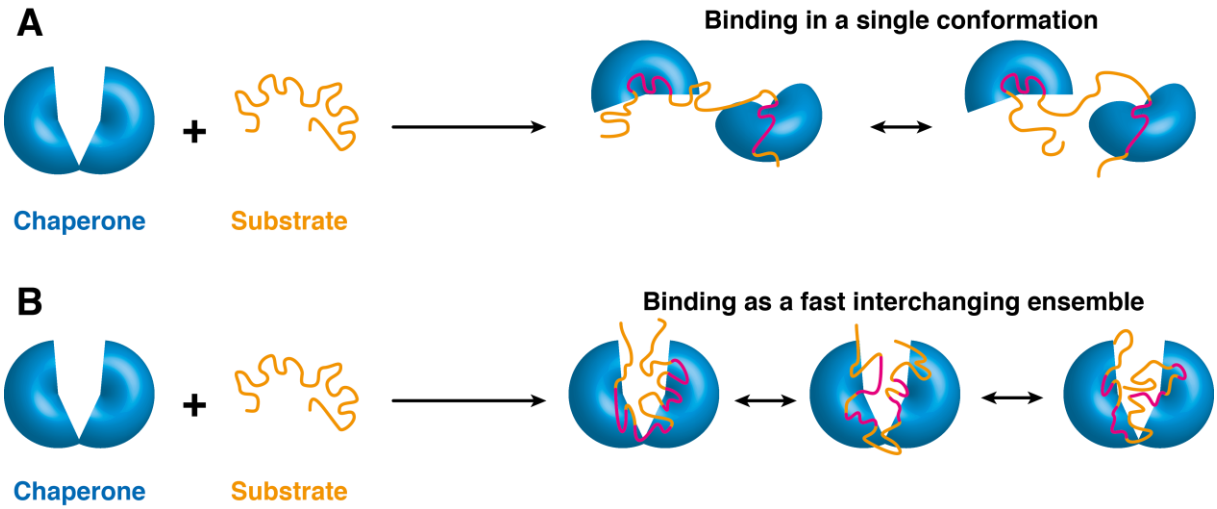

Fig. 2: Possible interaction modes between chaperones and their substrates. A) The substrate (orange) binds to the chaperone (blue) with well-defined interaction sites (magenta). While the non-interacting segments of the substrate can remain flexible, the chaperone-bound segments (magenta) adopt a well-defined structure. B) The substrate binds to the chaperone as an interchanging conformational ensemble. Segments of the substrate that are interacting with the chaperone at the initial time point (first conformer shown) are labeled magenta. These segments change their structure and interaction mode with the chaperone at other time points.

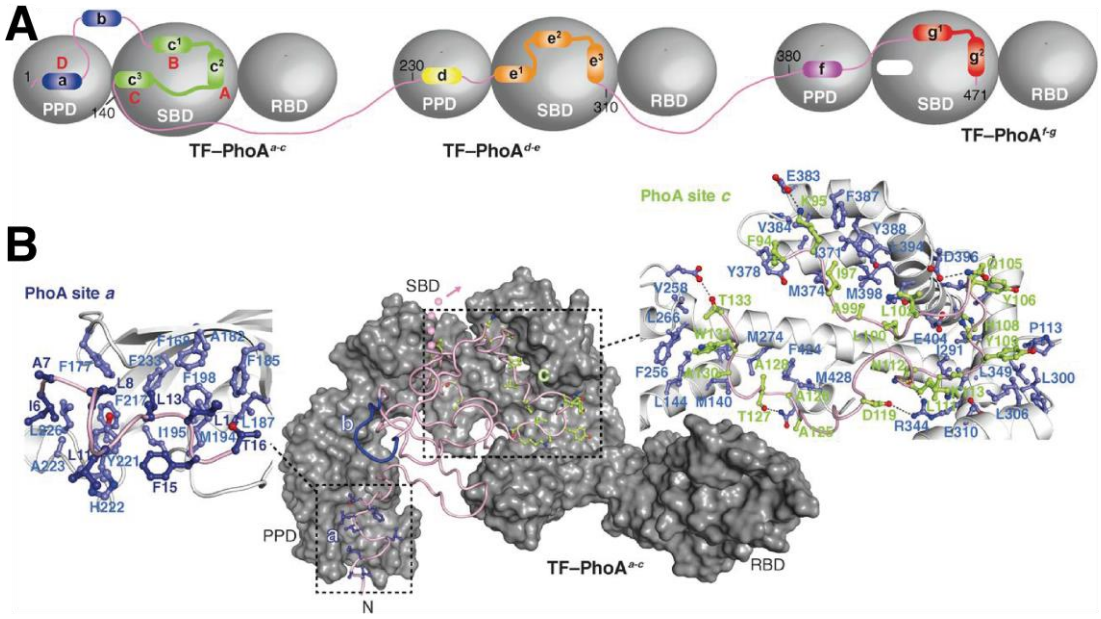

Fig. 3: Structural basis for the formation of the TF–PhoA complexes [91]. (A) Schematic for the interaction of PhoA with TF based on structural data. (B) Lowest-energy structure of one TF molecule in complex with the corresponding PhoA regions. TF is shown as a solvent-exposed surface and PhoA as a pink ribbon. The PhoA residues that directly interact with TF are drawn in a ball and stick representation. The pink arrows denote the direction of the PhoA chain, from the N- to the C-terminus. Close-up views of the structures are shown on the left for the PPD (site D) and on the right for the SBD (sites A, B, and C), bound to the corresponding PhoA sites. In the expanded views, the TF backbone is shown as a white cartoon and the PhoA backbone as a pink cartoon. The side chains of TF are colored blue, whereas the side chains of PhoA are colored green. The black broken lines denote hydrogen bonds that are formed in at least 70% of the conformers of the ensemble. Reprinted from Saio *et al*. [91] with permission from the authors and the American Association for the Advancement of Science.

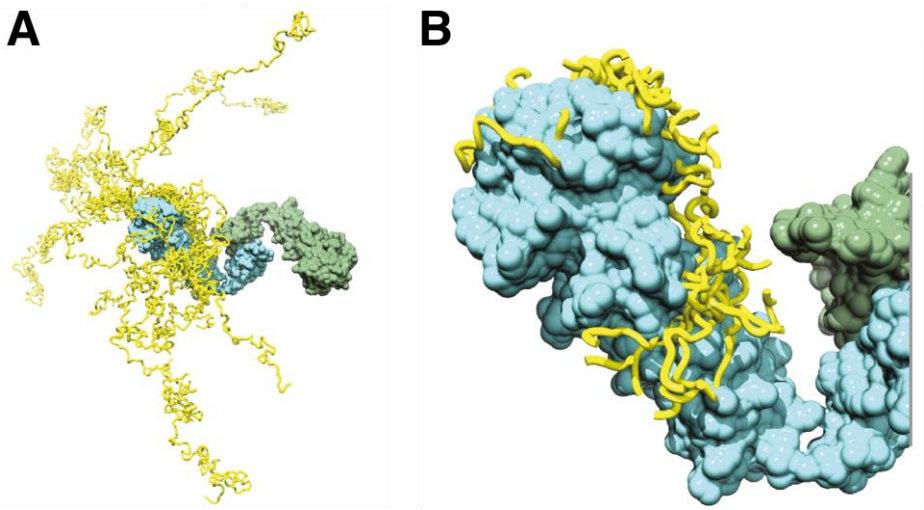

Fig. 4: Convergence of Tau models on Hsp90 based on SAXS data. (A) The ten best Tau models bound to Hsp90 (Tau models, yellow bands; Tau-binding Hsp90 protomer, cyan; other Hsp90 protomer, green). (B) The ten best Tau models within 10 Å of Hsp90 indicate convergence on Hsp90 (colors as in A). Reprinted from Karagöz *et al.* [192] with permission from the authors and Elsevier.

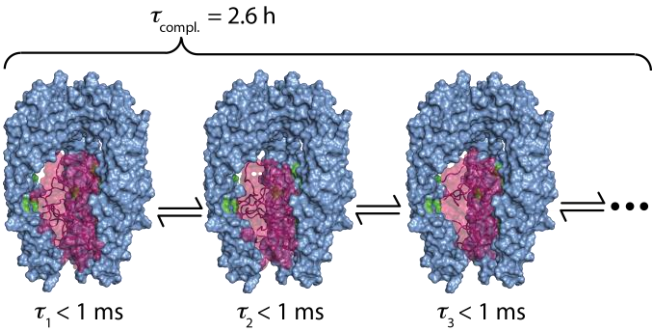

Fig. 5: Graphical representation of the conformational equilibrium of an Skp–OmpX complex. The complex is an ensemble of interconverting conformations in fast equilibrium with a global lifetime $\tau_{complex}$ of 2.6 h. Each individual conformation *i* has a lifetime τ_i of <1 ms. For this illustration, randomly generated OmpX polypeptide conformations (purple) were positioned within the Skp structure (blue) in surface representation (PDB ID 1SG2 [275]). Alanine residues in close spatial contact with methyl groups of OmpX are highlighted in green. Modified from Burmann *et al*. [84] and Callon *et al*. [85].

Tables

Table 1: Chaperone functions

Chaperone function	Description	Features	Examples
Holdase Chaperone	• Binds a non-natively folded substrate for sufficiently long lifetime to prevent aggregation in an energy-independent manner	• Does not influence the folded structure of the substrate protein • Keeps substrate in a folding-competent state • Release has to occur in an ATP-independent manner [84, 91, 373]	Skp, trigger factor, SecB, SurA
Translocase	• Mediates the trans-location of proteins across a membrane	• Can be energy-dependent or energy-independent [58, 59, 67]	SecYEG, TamA, Tom, FhaC
ATPase Chaperone	• Is involved in substrate folding and contains ATPase activity	• May use cycles of ATP consumption to facilitate folding of substrate proteins • May work in concert with auxiliary proteins [18, 24, 26]	DnaK, Hsp90
Chaperonin	• Encapsulates the substrate for energy-dependent folding	• Molecular complex composed of multiple subunits that assemble into double-ring structures • Competes kinetically on the pathway of misfolding and aggregation, thereby preventing aggregate formation [29]	GroEL/ES
Insertase	• Mediates the integration of proteins into a membrane	• Typically provides lateral access to the hydrophobic phase of the membrane • Can be energy-dependent or energy-independent [59, 67, 68, 325, 374]	SecYEG, YidC, BamA, TamA
Unfoldase	• Acts on misfolded proteins as substrates and unfolds them in an energy-dependent manner	• Alternates between high affinity and low affinity states to substrates in an ATP-dependent manner [18, 24] • Unfolded substrate proteins are released for chaperone-independent mediated transition to the native state [27]	DnaK, ClpX, ClpA
Disaggregase	• Resolves existing protein aggregates in an energy-dependent manner	• Works in conjunction with unfoldase proteins (e.g. DnaK) • Disaggregase function is energy-dependent [43, 44, 71, 243]	ClpB, Hsp104

Table 2: Overview of NMR techniques applied to molecular chaperones and protease machineries

	ATPase Chaperones		Holdase Chaperones				Unfoldases		Disaggregases	Proteases
		Chaperonins								
Method	Hsp90	GroEL/ES	Skp	Trigger factor	SecA	αB-crystallin	Hsp70/ Dnak	ClpX/ClpA	Hsp104/ClpB	Proteasome/ HslV/ClpP
Chemical shift perturbation	[102, 180, 181, 188, 189, 191, 192, 194, 204]	[211, 216-219, 222]	[84, 277]	[91]	[260, 266]	[313, 314]	[88, 123, 146, 151-154, 162]	[233, 235]	[48]	[236, 244, 245, 248-250, 253]
Spin relaxation	[187]	[224, 225]	[84, 277]	[91]	[263]	[300, 310, 311]	[121]		[48]	[236, 237, 246, 249]
Paramagnetic relaxation enhancement	[102, 181]		[84]		[260]	[304]			[48]	[245]
Transfer NOE	[189]	[137, 207, 208, 212, 217, 219]	[85]	[91]	[265]	[301]	[137, 140]		[94]	
Hydrogen/ deuterium exchange	[188]	[111-113, 209, 210, 218]					[149]			
Global lifetime measurement			[84]							
Determination of substrate compaction			[84]							
Residular dipolar couplings							[121-123]			
Exchange spectroscopy										[247]
Dark state saturation transfer		[109]								

References:

[1] F.U. Hartl, A. Bracher, M. Hayer-Hartl, Molecular chaperones in protein folding and proteostasis, Nature, 475 (2011) 324–332.
[2] B. Bukau, J. Weissman, A. Horwich, Molecular chaperones and protein quality control, Cell, 125 (2006) 443–451.
[3] Y.E. Kim, M.S. Hipp, A. Bracher, M. Hayer-Hartl, F.U. Hartl, Molecular chaperone functions in protein folding and proteostasis, Annu. Rev. Biochem., 82 (2013) 323–355.
[4] H.R. Saibil, Chaperone machines for protein folding, unfolding and disaggregation, Nat. Rev. Mol. Cell Biol., 14 (2013) 630–642.
[5] R. Rosenzweig, L.E. Kay, Bringing dynamic molecular machines into focus by methyl-TROSY NMR, Annu. Rev. Biochem., 83 (2014) 291-315.
[6] L.E. Kay, Solution NMR spectroscopy of supra-molecular systems, why bother? A methyl-TROSY view, J. Magn. Reson., 210 (2011) 159–170.
[7] C. Göbl, T. Madl, B. Simon, M. Sattler, NMR approaches for structural analysis of multidomain proteins and complexes in solution, Prog. Nucl. Magn. Reson. Spectrosc., 80 (2014) 26–63.
[8] C.B. Anfinsen, Principles that govern the folding of protein chains, Science, 181 (1973) 223–230.
[9] B.M. Burmann, S.H. Knauer, A. Sevostyanova, K. Schweimer, R.A. Mooney, R. Landick, I. Artsimovitch, P. Rösch, An α-helix to β-barrel domain switch transforms the transcription factor RfaH into a translation factor, Cell, 150 (2012) 291–303.
[10] R.L. Tuinstra, F.C. Peterson, S. Kutlesa, E.S. Elgin, M.A. Kron, B.F. Volkman, Interconversion between two unrelated protein folds in the lymphotactin native state, Proc. Natl. Acad. Sci. USA, 105 (2008) 5057–5062.
[11] X. Luo, R. Yu, Protein Metamorphosis: The two-state behavior of Mad2, Structure, 16 (2008) 1616–1625.
[12] R.J. Ellis, Molecular chaperones: the plant connection, Science, 250 (1990) 954–959.
[13] R.J. Ellis, Proteins as molecular chaperones, Nature, 328 (1987) 378–379.
[14] R.J. Ellis, S.M. van der Vies, Molecular chaperones, Annu. Rev. Biochem., 60 (1991) 321–347.
[15] R.J. Ellis, S.M. Hemmingsen, Molecular chaperones: proteins essential for the biogenesis of some macromolecular structures, Trends Biochem. Sci., 14 (1989) 339–342.
[16] J.E. Rothman, Polypeptide chain binding proteins: catalysts of protein folding and related processes in cells, Cell, 59 (1989) 591–601.
[17] F.U. Hartl, J. Martin, Molecular chaperones in cellular protein folding, Curr. Opin. Struct. Biol., 5 (1995) 92–102.
[18] S.V. Slepenkov, S.N. Witt, The unfolding story of the *Escherichia coli* Hsp70 DnaK: is DnaK a holdase or an unfoldase?, Mol. Microbiol., 45 (2002) 1197–1206.
[19] L. Ferbitz, T. Maier, H. Patzelt, B. Bukau, E. Deuerling, N. Ban, Trigger factor in complex with the ribosome forms a molecular cradle for nascent proteins, Nature, 431 (2004) 590–596.

[20] F. Merz, D. Boehringer, C. Schaffitzel, S. Preissler, A. Hoffmann, T. Maier, A. Rutkowska, J. Lozza, N. Ban, B. Bukau, E. Deuerling, Molecular mechanism and structure of Trigger Factor bound to the translating ribosome, EMBO J., 27 (2008) 1622–1632.
[21] E.P. O'Brian, J. Christodoulou, M. Vendruscolo, C.M. Dobson, Trigger factor slows co-translational folding through kinetic trapping while sterically protecting the nascent chain from aberrant cytosolic interactions, J. Am. Chem. Soc., 134 (2012) 10920–10932.
[22] E. Barbet-Massin, C.T. Huang, V. Daebel, S.T. Hsu, B. Reif, Site-specific solid-state NMR studies of "Trigger Factor" in complex with the large ribosomal subunit 50S, Angew. Chem. Int. Ed. Engl., (2015) in press.
[23] C.L. Hagan, T.J. Silhavy, D. Kahne, β-Barrel membrane protein assembly by the Bam complex, Annu. Rev. Biochem., 80 (2011) 189–210.
[24] B. Bukau, E. Deuerling, C. Pfund, E.A. Craig, Getting newly synthesized proteins into shape, Cell, 101 (2000) 119–122.
[25] M.P. Mayer, Gymnastics of molecular chaperones, Mol. Cell, 39 (2010) 321–331.
[26] J. Li, J. Soroka, J. Buchner, The Hsp90 chaperone machinery: conformational dynamics and regulation by co-chaperones, Biochim. Biophys. Acta, 1823 (2012) 624–635.
[27] S.K. Sharma, P. De los Rios, P. Christen, A. Lustig, P. Goloubinoff, The kinetic parameters and energy cost of the Hsp70 chaperone as a polypeptide unfoldase, Nat. Chem. Biol., 6 (2010) 914–920.
[28] A.L. Horwich, W.A. Fenton, E. Chapman, G.W. Farr, Two families of chaperonin: physiology and mechanism, Annu. Rev. Cell. Dev. Biol., 23 (2007) 115–145.
[29] A.L. Horwich, W.A. Fenton, Chaperonin-mediated protein folding: using a central cavity to kinetically assist polypeptide chain folding, Q. Rev. Biophys., 42 (2009) 83–116.
[30] F.U. Hartl, Molecular chaperones in cellular protein folding, Nature, 381 (1996) 571–579.
[31] F. Georgescauld, K. Popova, A.J. Gupta, A. Bracher, J.R. Engen, M. Hayer-Hartl, F.U. Hartl, GroEL/ES chaperonin modulates the mechanism and accelerates the rate of TIM-barrel domain folding, Cell, 157 (2014) 922–934.
[32] M.J. Kerner, D.J. Naylor, Y. Ishihama, T. Maier, H.C. Chang, A.P. Stines, C. Georgopoulos, D. Frishman, M. Hayer-Hartl, M. Mann, F.U. Hartl, Proteome-wide analysis of chaperonin-dependent protein folding in *Escherichia coli*, Cell, 122 (2005) 209–220.
[33] M.M. Gromiha, S. Selvaraj, Inter-residue interactions in protein folding and stability, Prog. Biophys. Mol. Biol., 86 (2004) 235–277.
[34] Z. Xu, A.L. Horwich, P.B. Sigler, The crystal structure of the asymmetric GroEL-GroES-$(ADP)_7$ chaperonin complex, Nature, 388 (1997) 741–750.
[35] R.T. Sauer, T.A. Baker, AAA+ proteases: ATP-fueled machines of protein destruction, Annu. Rev. Biochem., 80 (2011) 587–612.
[36] J. Hinnerwisch, W.A. Fenton, K.J. Furtak, G.W. Farr, A.L. Horwich, Loops in the central channel of ClpA chaperone mediate protein binding, unfolding, and translocation, Cell, 121 (2005) 1029–1041.
[37] R.T. Sauer, D.N. Bolon, B.M. Burton, R.E. Burton, J.M. Flynn, R.A. Grant, G.L. Hersch, S.A. Joshi, J.A. Kenniston, I. Levchenko, S.B. Neher, E.S. Oakes, S.M. Siddiqui, D.A. Wah, T.A. Baker, Sculpting the proteome with AAA+ proteases and disassembly machines, Cell, 119 (2004) 9–18.
[38] T.A. Baker, R.T. Sauer, ATP-dependent proteases of bacteria: recognition logic and operating principles, Trends Biochem. Sci., 31 (2006) 647–653.

[39] S.E. Glynn, A. Martin, A.R. Nager, T.A. Baker, R.T. Sauer, Structures of asymmetric ClpX hexamers reveal nucleotide-dependent motions in a AAA+ protein-unfolding machine, Cell, 139 (2009) 744–756.
[40] R.A. Maillard, G. Chistol, M. Sen, M. Righini, J. Tan, C.M. Kaiser, C. Hodges, A. Martin, C. Bustamante, ClpX(P) generates mechanical force to unfold and translocate its protein substrates, Cell, 145 (2011) 459–469.
[41] M. Sen, R.A. Maillard, K. Nyquist, P. Rodriguez-Aliaga, S. Presse, A. Martin, C. Bustamante, The ClpXP protease unfolds substrates using a constant rate of pulling but different gears, Cell, 155 (2013) 636–646.
[42] R. Kellner, H. Hofmann, A. Barducci, B. Wunderlich, D. Nettels, B. Schuler, Single-molecule spectroscopy reveals chaperone-mediated expansion of substrate protein, Proc. Natl. Acad. Sci. USA, 111 (2014) 13355–13360.
[43] S.M. Doyle, O. Genest, S. Wickner, Protein rescue from aggregates by powerful molecular chaperone machines, Nat. Rev. Mol. Cell Biol., 14 (2013) 617–629.
[44] A. Mogk, B. Bukau, Molecular chaperones: structure of a protein disaggregase, Curr. Biol., 14 (2004) 78–80.
[45] S. Lee, M.E. Sowa, Y.H. Watanabe, P.B. Sigler, W. Chiu, M. Yoshida, F.T. Tsai, The structure of ClpB: a molecular chaperone that rescues proteins from an aggregated state, Cell, 115 (2003) 229–240.
[46] J. Weibezahn, P. Tessarz, C. Schlieker, R. Zahn, Z. Maglica, S. Lee, H. Zentgraf, E.U. Weber-Ban, D.A. Dougan, F.T. Tsai, A. Mogk, B. Bukau, Thermotolerance requires refolding of aggregated proteins by substrate translocation through the central pore of ClpB, Cell, 119 (2004) 653–665.
[47] F. Seyffer, E. Kummer, Y. Oguchi, J. Winkler, M. Kumar, R. Zahn, V. Sourjik, B. Bukau, A. Mogk, Hsp70 proteins bind Hsp100 regulatory M domains to activate AAA+ disaggregase at aggregate surfaces, Nat. Struct. Mol. Biol., 19 (2012) 1347–1355.
[48] R. Rosenzweig, S. Moradi, A. Zarrine-Afsar, J.R. Glover, L.E. Kay, Unraveling the mechanism of protein disaggregation through a ClpB-DnaK interaction, Science, 339 (2013) 1080–1083.
[49] S.P. Acebron, V. Fernandez-Saiz, S.G. Taneva, F. Moro, A. Muga, DnaJ recruits DnaK to protein aggregates, J. Biol. Chem., 283 (2008) 1381–1390.
[50] J. Winkler, J. Tyedmers, B. Bukau, A. Mogk, Hsp70 targets Hsp100 chaperones to substrates for protein disaggregation and prion fragmentation, J. Cell Biol., 198 (2012) 387–404.
[51] S. Zietkiewicz, A. Lewandowska, P. Stocki, K. Liberek, Hsp70 chaperone machine remodels protein aggregates at the initial step of Hsp70-Hsp100-dependent disaggregation, J. Biol. Chem., 281 (2006) 7022–7029.
[52] S.P. Acebron, I. Martin, U. del Castillo, F. Moro, A. Muga, DnaK-mediated association of ClpB to protein aggregates. A bichaperone network at the aggregate surface, FEBS Lett., 583 (2009) 2991–2996.
[53] P. Tessarz, A. Mogk, B. Bukau, Substrate threading through the central pore of the Hsp104 chaperone as a common mechanism for protein disaggregation and prion propagation, Mol. Microbiol., 68 (2008) 87–97.
[54] C. Schlieker, J. Weibezahn, H. Patzelt, P. Tessarz, C. Strub, K. Zeth, A. Erbse, J. Schneider-Mergener, J.W. Chin, P.G. Schultz, B. Bukau, A. Mogk, Substrate recognition by the AAA+ chaperone ClpB, Nat. Struct. Mol. Biol., 11 (2004) 607–615.
[55] R. Lum, J.M. Tkach, E. Vierling, J.R. Glover, Evidence for an unfolding/threading mechanism for protein disaggregation by *Saccharomyces cerevisiae* Hsp104, J. Biol. Chem., 279 (2004) 29139–29146.

[56] T.A. Rapoport, B. Jungnickel, U. Kutay, Protein transport across the eukaryotic endoplasmic reticulum and bacterial inner membranes, Annu. Rev. Biochem., 65 (1996) 271–303.
[57] A.J. Driessen, N. Nouwen, Protein translocation across the bacterial cytoplasmic membrane, Annu. Rev. Biochem., 77 (2008) 643–667.
[58] W. Neupert, J.M. Herrmann, Translocation of proteins into mitochondria, Annu. Rev. Biochem., 76 (2007) 723–749.
[59] A.N.J.A. Lycklama, A.J. Driessen, The bacterial Sec-translocase: structure and mechanism, Philos. Trans. R. Soc. Lond. B Biol. Sci., 367 (2012) 1016–1028.
[60] E. Schleiff, T. Becker, Common ground for protein translocation: access control for mitochondria and chloroplasts, Nat. Rev. Mol. Cell Biol., 12 (2011) 48–59.
[61] B. Clantin, A.S. Delattre, P. Rucktooa, N. Saint, A.C. Meli, C. Locht, F. Jacob-Dubuisson, V. Villeret, Structure of the membrane protein FhaC: a member of the Omp85-TpsB transporter superfamily, Science, 317 (2007) 957–961.
[62] B. Van den Berg, W.M. Clemons, Jr., I. Collinson, Y. Modis, E. Hartmann, S.C. Harrison, T.A. Rapoport, X-ray structure of a protein-conducting channel, Nature, 427 (2004) 36–44.
[63] R.E. Dalbey, P. Wang, A. Kuhn, Assembly of bacterial inner membrane proteins, Annu. Rev. Biochem., 80 (2011) 161–187.
[64] N. Noinaj, A.J. Kuszak, J.C. Gumbart, P. Lukacik, H. Chang, N.C. Easley, T. Lithgow, S.K. Buchanan, Structural insight into the biogenesis of β-barrel membrane proteins, Nature, 501 (2013) 385–390.
[65] R. Albrecht, M. Schütz, P. Oberhettinger, M. Faulstich, I. Bermejo, T. Rudel, K. Diederichs, K. Zeth, Structure of BamA, an essential factor in outer membrane protein biogenesis, Acta Crystallogr. D Biol. Crystallogr., 70 (2014) 1779–1789.
[66] D. Ni, Y. Wang, X. Yang, H. Zhou, X. Hou, B. Cao, Z. Lu, X. Zhao, K. Yang, Y. Huang, Structural and functional analysis of the β-barrel domain of BamA from *Escherichia coli*, FASEB J., 28 (2014) 2677–2685.
[67] F. Gruss, F. Zähringer, R.P. Jakob, B.M. Burmann, S. Hiller, T. Maier, The structural basis of autotransporter translocation by TamA, Nat. Struct. Mol. Biol., 20 (2013) 1318–1320.
[68] N. Noinaj, A.J. Kuszak, C. Balusek, J.C. Gumbart, S.K. Buchanan, Lateral opening and exit pore formation are required for BamA function, Structure, 22 (2014) 1055–1062.
[69] D. Gessmann, Y.H. Chung, E.J. Danoff, A.M. Plummer, C.W. Sandlin, N.R. Zaccai, K.G. Fleming, Outer membrane β-barrel protein folding is physically controlled by periplasmic lipid head groups and BamA, Proc. Natl. Acad. Sci. USA, 111 (2014) 5878–5883.
[70] T. Inobe, A. Matouschek, Protein targeting to ATP-dependent proteases, Curr. Opin. Struct. Biol., 18 (2008) 43–51.
[71] M. Bochtler, C. Hartmann, H.K. Song, G.P. Bourenkov, H.D. Bartunik, R. Huber, The structures of HsIU and the ATP-dependent protease HsIU-HsIV, Nature, 403 (2000) 800–805.
[72] M.C. Sousa, C.B. Trame, H. Tsuruta, S.M. Wilbanks, V.S. Reddy, D.B. McKay, Crystal and solution structures of an HslUV protease-chaperone complex, Cell, 103 (2000) 633–643.
[73] J. Wang, J.A. Hartling, J.M. Flanagan, The structure of ClpP at 2.3 Å resolution suggests a model for ATP-dependent proteolysis, Cell, 91 (1997) 447–456.

[74] J. Löwe, D. Stock, B. Jap, P. Zwickl, W. Baumeister, R. Huber, Crystal structure of the 20S proteasome from the archaeon *T. acidophilum* at 3.4 Å resolution, Science, 268 (1995) 533–539.
[75] A. Förster, E.I. Masters, F.G. Whitby, H. Robinson, C.P. Hill, The 1.9 Å structure of a proteasome-11S activator complex and implications for proteasome-PAN/PA700 interactions, Mol. Cell, 18 (2005) 589–599.
[76] W. Baumeister, J. Walz, F. Zühl, E. Seemüller, The proteasome: paradigm of a self-compartmentalizing protease, Cell, 92 (1998) 367–380.
[77] C.N. Larsen, D. Finley, Protein translocation channels in the proteasome and other proteases, Cell, 91 (1997) 431–434.
[78] J. Rabl, D.M. Smith, Y. Yu, S.C. Chang, A.L. Goldberg, Y. Cheng, Mechanism of gate opening in the 20S proteasome by the proteasomal ATPases, Mol. Cell, 30 (2008) 360–368.
[79] G. Effantin, M.R. Maurizi, A.C. Steven, Binding of the ClpA unfoldase opens the axial gate of ClpP peptidase, J. Biol. Chem., 285 (2010) 14834–14840.
[80] M.E. Lee, T.A. Baker, R.T. Sauer, Control of substrate gating and translocation into ClpP by channel residues and ClpX binding, J. Mol. Biol., 399 (2010) 707–718.
[81] A.F. Kisselev, T.N. Akopian, K.M. Woo, A.L. Goldberg, The sizes of peptides generated from protein by mammalian 26 and 20 S proteasomes. Implications for understanding the degradative mechanism and antigen presentation, J. Biol. Chem., 274 (1999) 3363–3371.
[82] R. Grimaud, M. Kessel, F. Beuron, A.C. Steven, M.R. Maurizi, Enzymatic and structural similarities between the *Escherichia coli* ATP-dependent proteases, ClpXP and ClpAP, J. Biol. Chem., 273 (1998) 12476–12481.
[83] D. Missiakas, F. Schwager, J.M. Betton, C. Georgopoulos, S. Raina, Identification and characterization of HsIV HsIU (ClpQ ClpY) proteins involved in overall proteolysis of misfolded proteins in *Escherichia coli*, EMBO J., 15 (1996) 6899–6909.
[84] B.M. Burmann, C. Wang, S. Hiller, Conformation and dynamics of the periplasmic membrane-protein–chaperone complexes OmpX-Skp and tOmpA-Skp, Nat. Struct. Mol. Biol., 20 (2013) 1265–1272.
[85] M. Callon, B.M. Burmann, S. Hiller, Structural mapping of a chaperone–substrate interaction surface, Angew. Chem. Int. Ed. Engl., 53 (2014) 5069–5072.
[86] M.P. Williamson, Using chemical shift perturbation to characterise ligand binding, Prog. Nucl. Magn. Reson. Spectrosc., 73 (2013) 1–16.
[87] D.S. Wishart, Interpreting protein chemical shift data, Prog. Nucl. Magn. Reson. Spectrosc., 58 (2011) 62–87.
[88] A. Zhuravleva, E.M. Clerico, L.M. Gierasch, An interdomain energetic tug-of-war creates the allosterically active state in Hsp70 molecular chaperones, Cell, 151 (2012) 1296–1307.
[89] G. Manley, J.P. Loria, NMR insights into protein allostery, Arch. Biochem. Biophys., 519 (2012) 223–231.
[90] E.R. Zuiderweg, Mapping protein-protein interactions in solution by NMR spectroscopy, Biochemistry, 41 (2002) 1–7.
[91] T. Saio, X. Guan, P. Rossi, A. Economou, C.G. Kalodimos, Structural basis for protein antiaggregation activity of the trigger factor chaperone, Science, 344 (2014) 1250494.
[92] K. Wüthrich, NMR of Proteins and Nucleic Acids, Wiley, New York, 1986.
[93] M. Mayer, B. Meyer, Characterization of ligand binding by saturation transfer difference NMR spectroscopy, Angew. Chem. Int. Ed. Engl., 38 (1999) 1784–1788.

[94] S. Narayanan, B. Bosl, S. Walter, B. Reif, Importance of low-oligomeric-weight species for prion propagation in the yeast prion system Sup35/Hsp104, Proc. Natl. Acad. Sci. USA, 100 (2003) 9286–9291.
[95] G. Otting, Protein NMR using paramagnetic ions, Annu. Rev. Biophys., 39 (2010) 387–405.
[96] P.H. Keizers, M. Ubbink, Paramagnetic tagging for protein structure and dynamics analysis, Prog. Nucl. Magn. Reson. Spectrosc., 58 (2011) 88–96.
[97] I. Bertini, C. Luchinat, G. Parigi, Magnetic susceptibility in paramagnetic NMR, Prog. Nucl. Magn. Reson. Spectrosc., 40 (2002) 249–273.
[98] J.L. Battiste, G. Wagner, Utilization of site-directed spin labeling and high-resolution heteronuclear nuclear magnetic resonance for global fold determination of large proteins with limited nuclear overhauser effect data, Biochemistry, 39 (2000) 5355–5365.
[99] G.M. Clore, J. Iwahara, Theory, practice, and applications of paramagnetic relaxation enhancement for the characterization of transient low-population states of biological macromolecules and their complexes, Chem. Rev., 109 (2009) 4108–4139.
[100] G. Pintacuda, M. John, X.C. Su, G. Otting, NMR structure determination of protein-ligand complexes by lanthanide labeling, Acc. Chem. Res., 40 (2007) 206–212.
[101] I. Bertini, M.B. Janik, Y.M. Lee, C. Luchinat, A. Rosato, Magnetic susceptibility tensor anisotropies for a lanthanide ion series in a fixed protein matrix, J. Am. Chem. Soc., 123 (2001) 4181–4188.
[102] F. Hagn, S. Lagleder, M. Retzlaff, J. Rohrberg, O. Demmer, K. Richter, J. Buchner, H. Kessler, Structural analysis of the interaction between Hsp90 and the tumor suppressor protein p53, Nat. Struct. Mol. Biol., 18 (2011) 1086–1093.
[103] A.G. Palmer, 3rd, C.D. Kroenke, J.P. Loria, Nuclear magnetic resonance methods for quantifying microsecond-to-millisecond motions in biological macromolecules, Methods Enzymol., 339 (2001) 204–238.
[104] H.J. Dyson, P.E. Wright, Nuclear magnetic resonance methods for elucidation of structure and dynamics in disordered states, Methods Enzymol., 339 (2001) 258–270.
[105] A. Mittermaier, L.E. Kay, New tools provide new insights in NMR studies of protein dynamics, Science, 312 (2006) 224–228.
[106] A.G. Palmer, 3rd, NMR characterization of the dynamics of biomacromolecules, Chem. Rev., 104 (2004) 3623–3640.
[107] N.L. Fawzi, J. Ying, R. Ghirlando, D.A. Torchia, G.M. Clore, Atomic-resolution dynamics on the surface of amyloid-β protofibrils probed by solution NMR, Nature, 480 (2011) 268–272.
[108] N.L. Fawzi, J. Ying, D.A. Torchia, G.M. Clore, Probing exchange kinetics and atomic resolution dynamics in high-molecular-weight complexes using dark-state exchange saturation transfer NMR spectroscopy, Nat. Protoc., 7 (2012) 1523–1533.
[109] D.S. Libich, N.L. Fawzi, J. Ying, G.M. Clore, Probing the transient dark state of substrate binding to GroEL by relaxation-based solution NMR, Proc. Natl. Acad. Sci. USA, 110 (2013) 11361–11366.
[110] S.W. Englander, L. Mayne, Protein folding studied using hydrogen-exchange labeling and two-dimensional NMR, Annu. Rev. Biophys. Biomol. Struct., 21 (1992) 243–265.
[111] R. Horst, W.A. Fenton, S.W. Englander, K. Wüthrich, A.L. Horwich, Folding trajectories of human dihydrofolate reductase inside the GroEL–GroES chaperonin cavity and free in solution, Proc. Natl. Acad. Sci. USA, 104 (2007) 20788–20792.

[112] M.S. Goldberg, J. Zhang, S. Sondek, C.R. Matthews, R.O. Fox, A.L. Horwich, Native-like structure of a protein-folding intermediate bound to the chaperonin GroEL, Proc. Natl. Acad. Sci. USA, 94 (1997) 1080–1085.
[113] R. Zahn, C. Spitzfaden, M. Ottiger, K. Wüthrich, A. Plückthun, Destabilization of the complete protein secondary structure on binding to the chaperone GroEL, Nature, 368 (1994) 261–265.
[114] A. Mainz, S. Jehle, B.J. van Rossum, H. Oschkinat, B. Reif, Large protein complexes with extreme rotational correlation times investigated in solution by magic-angle-spinning NMR spectroscopy, J. Am. Chem. Soc., 131 (2009) 15968–15969.
[115] A. Mainz, T.L. Religa, R. Sprangers, R. Linser, L.E. Kay, B. Reif, NMR spectroscopy of soluble protein complexes at one mega-dalton and beyond, Angew. Chem. Int. Ed. Engl., 52 (2013) 8746–8751.
[116] A. Mainz, B. Bardiaux, F. Kuppler, G. Multhaup, I.C. Felli, R. Pierattelli, B. Reif, Structural and mechanistic implications of metal binding in the small heat-shock protein αB-crystallin, J. Biol. Chem., 287 (2012) 1128–1138.
[117] I. Bertini, C. Luchinat, G. Parigi, E. Ravera, B. Reif, P. Turano, Solid-state NMR of proteins sedimented by ultracentrifugation, Proc. Natl. Acad. Sci. USA, 108 (2011) 10396–10399.
[118] S. Jehle, P. Rajagopal, B. Bardiaux, S. Markovic, R. Kühne, J.R. Stout, V.A. Higman, R.E. Klevit, B.J. van Rossum, H. Oschkinat, Solid-state NMR and SAXS studies provide a structural basis for the activation of αB-crystallin oligomers, Nat. Struct. Mol. Biol., 17 (2010) 1037–1042.
[119] M. Blackledge, Recent progress in the study of biomolecular structure and dynamics in solution from residual dipolar couplings, Prog. Nucl. Magn. Reson. Spectrosc., 46 (2005) 23–61.
[120] A. Bax, G. Kontaxis, N. Tjandra, Dipolar couplings in macromolecular structure determination, Methods Enzymol., 339 (2001) 127–174.
[121] E.B. Bertelsen, L. Chang, J.E. Gestwicki, E.R. Zuiderweg, Solution conformation of wild-type *E. coli* Hsp70 (DnaK) chaperone complexed with ADP and substrate, Proc. Natl. Acad. Sci. USA, 106 (2009) 8471–8476.
[122] A. Bhattacharya, A.V. Kurochkin, G.N. Yip, Y. Zhang, E.B. Bertelsen, E.R. Zuiderweg, Allostery in Hsp70 chaperones is transduced by subdomain rotations, J. Mol. Biol., 388 (2009) 475–490.
[123] M. Revington, Y. Zhang, G.N. Yip, A.V. Kurochkin, E.R. Zuiderweg, NMR investigations of allosteric processes in a two-domain *Thermus thermophilus* Hsp70 molecular chaperone, J. Mol. Biol., 349 (2005) 163–183.
[124] T. Maier, L. Ferbitz, E. Deuerling, N. Ban, A cradle for new proteins: trigger factor at the ribosome, Curr. Opin. Struct. Biol., 15 (2005) 204–212.
[125] A.V. Ludlam, B.A. Moore, Z. Xu, The crystal structure of ribosomal chaperone trigger factor from *Vibrio cholerae*, Proc. Natl. Acad. Sci. USA, 101 (2004) 13436–13441.
[126] F.X. Schmid, L.M. Mayr, M. Mücke, E.R. Schönbrunner, Prolyl isomerases: role in protein folding, Adv. Protein Chem., 44 (1993) 25–66.
[127] H. Patzelt, G. Kramer, T. Rauch, H.J. Schönfeld, B. Bukau, E. Deuerling, Three-state equilibrium of *Escherichia coli* trigger factor, Biol. Chem., 383 (2002) 1611–1619.
[128] E. Oh, A.H. Becker, A. Sandikci, D. Huber, R. Chaba, F. Gloge, R.J. Nichols, A. Typas, C.A. Gross, G. Kramer, J.S. Weissman, B. Bukau, Selective ribosome profiling reveals the cotranslational chaperone action of trigger factor *in vivo*, Cell, 147 (2011) 1295–1308.

[129] T.N. Parac, M. Vogtherr, M. Maurer, A. Pahl, H. Rüterjansl, C. Griesinger, K. Fiebig, Assignment of the ^{1}H, ^{13}C and ^{15}N resonances of the PPIase domain of the trigger factor from *Mycoplasma genitalium*, J. Biomol. NMR, 20 (2001) 193–194.
[130] M. Vogtherr, D.M. Jacobs, T.N. Parac, M. Maurer, A. Pahl, K. Saxena, H. Rüterjans, C. Griesinger, K.M. Fiebig, NMR solution structure and dynamics of the peptidyl-prolyl cis-trans isomerase domain of the trigger factor from *Mycoplasma genitalium* compared to FK506-binding protein, J. Mol. Biol., 318 (2002) 1097–1115.
[131] O. Kristensen, M. Gajhede, Chaperone binding at the ribosomal exit tunnel, Structure, 11 (2003) 1547–1556.
[132] S.T. Hsu, C.M. Dobson, ^{1}H, ^{15}N and ^{13}C assignments of the dimeric ribosome binding domain of trigger factor from *Escherichia coli*, Biomol. NMR Assign., 3 (2009) 17–20.
[133] E. Martinez-Hackert, W.A. Hendrickson, Structures of and interactions between domains of trigger factor from *Thermotoga maritima*, Acta Crystallogr. D Biol. Crystallogr., 63 (2007) 536–547.
[134] Y. Yao, G. Bhabha, G. Kroon, M. Landes, H.J. Dyson, Structure discrimination for the C-terminal domain of *Escherichia coli* trigger factor in solution, J. Biomol. NMR, 40 (2008) 23–30.
[135] H.H. Kampinga, E.A. Craig, The HSP70 chaperone machinery: J proteins as drivers of functional specificity, Nat. Rev. Mol. Cell Biol., 11 (2010) 579–592.
[136] E.R. Zuiderweg, E.B. Bertelsen, A. Rousaki, M.P. Mayer, J.E. Gestwicki, A. Ahmad, Allostery in the Hsp70 chaperone proteins, Top. Curr. Chem., 328 (2013) 99–153.
[137] S.J. Landry, R. Jordan, R. McMacken, L.M. Gierasch, Different conformations for the same polypeptide bound to chaperones DnaK and GroEL, Nature, 355 (1992) 455–457.
[138] R.C. Morshauser, H. Wang, G.C. Flynn, E.R. Zuiderweg, The peptide-binding domain of the chaperone protein Hsc70 has an unusual secondary structure topology, Biochemistry, 34 (1995) 6261–6266.
[139] K.M. Flaherty, C. DeLuca-Flaherty, D.B. McKay, Three-dimensional structure of the ATPase fragment of a 70K heat-shock cognate protein, Nature, 346 (1990) 623–628.
[140] S. Cai, S.Y. Stevens, A.P. Budor, E.R. Zuiderweg, Solvent interaction of a Hsp70 chaperone substrate-binding domain investigated with water-NOE NMR experiments, Biochemistry, 42 (2003) 11100–11108.
[141] S.Y. Stevens, S. Cai, M. Pellecchia, E.R. Zuiderweg, The solution structure of the bacterial HSP70 chaperone protein domain DnaK(393-507) in complex with the peptide NRLLLTG, Protein Sci., 12 (2003) 2588-2596.
[142] W.F. Burkholder, X. Zhao, X. Zhu, W.A. Hendrickson, A. Gragerov, M.E. Gottesman, Mutations in the C-terminal fragment of DnaK affecting peptide binding, Proc. Natl. Acad. Sci. USA, 93 (1996) 10632–10637.
[143] C. Voisine, E.A. Craig, N. Zufall, O. von Ahsen, N. Pfanner, W. Voos, The protein import motor of mitochondria: unfolding and trapping of preproteins are distinct and separable functions of matrix Hsp70, Cell, 97 (1999) 565–574.
[144] M. Pellecchia, D.L. Montgomery, S.Y. Stevens, C.W. Vander Kooi, H.P. Feng, L.M. Gierasch, E.R. Zuiderweg, Structural insights into substrate binding by the molecular chaperone DnaK, Nat. Struct. Biol., 7 (2000) 298–303.
[145] M. Revington, E.R. Zuiderweg, TROSY-driven NMR backbone assignments of the 381-residue nucleotide-binding domain of the *Thermus Thermophilus* DnaK molecular chaperone, J. Biomol. NMR, 30 (2004) 113–114.
[146] M. Revington, T.M. Holder, E.R. Zuiderweg, NMR study of nucleotide-induced changes in the nucleotide binding domain of *Thermus thermophilus* Hsp70 chaperone

DnaK: implications for the allosteric mechanism, J. Biol. Chem., 279 (2004) 33958–33967.
[147] B.F. Volkman, D. Lipson, D.E. Wemmer, D. Kern, Two-state allosteric behavior in a single-domain signaling protein, Science, 291 (2001) 2429–2433.
[148] D. Kern, E.R. Zuiderweg, The role of dynamics in allosteric regulation, Curr. Opin. Struct. Biol., 13 (2003) 748–757.
[149] J.F. Swain, E.G. Schulz, L.M. Gierasch, Direct comparison of a stable isolated Hsp70 substrate-binding domain in the empty and substrate-bound states, J. Biol. Chem., 281 (2006) 1605–1611.
[150] J.F. Swain, R. Sivendran, L.M. Gierasch, Defining the structure of the substrate-free state of the DnaK molecular chaperone, Biochem. Soc. Symp., (2001) 69-82.
[151] A. Zhuravleva, L.M. Gierasch, Allosteric signal transmission in the nucleotide-binding domain of 70-kDa heat shock protein (Hsp70) molecular chaperones, Proc. Natl. Acad. Sci. USA, 108 (2011) 6987–6992.
[152] S. Wisen, E.B. Bertelsen, A.D. Thompson, S. Patury, P. Ung, L. Chang, C.G. Evans, G.M. Walter, P. Wipf, H.A. Carlson, J.L. Brodsky, E.R. Zuiderweg, J.E. Gestwicki, Binding of a small molecule at a protein-protein interface regulates the chaperone activity of Hsp70-Hsp40, ACS Chem. Biol., 5 (2010) 611–622.
[153] A. Rousaki, Y. Miyata, U.K. Jinwal, C.A. Dickey, J.E. Gestwicki, E.R. Zuiderweg, Allosteric drugs: the interaction of antitumor compound MKT-077 with human Hsp70 chaperones, J. Mol. Biol., 411 (2011) 614–632.
[154] U.K. Jinwal, E. Akoury, J.F. Abisambra, J.C. O'Leary, 3rd, A.D. Thompson, L.J. Blair, Y. Jin, J. Bacon, B.A. Nordhues, M. Cockman, J. Zhang, P. Li, B. Zhang, S. Borysov, V.N. Uversky, J. Biernat, E. Mandelkow, J.E. Gestwicki, M. Zweckstetter, C.A. Dickey, Imbalance of Hsp70 family variants fosters tau accumulation, FASEB J., 27 (2013) 1450–1459.
[155] T. Szyperski, M. Pellecchia, D. Wall, C. Georgopoulos, K. Wüthrich, NMR structure determination of the *Escherichia coli* DnaJ molecular chaperone: secondary structure and backbone fold of the N-terminal region (residues 2-108) containing the highly conserved J domain, Proc. Natl. Acad. Sci. USA, 91 (1994) 11343–11347.
[156] M. Pellecchia, T. Szyperski, D. Wall, C. Georgopoulos, K. Wüthrich, NMR structure of the J-domain and the Gly/Phe-rich region of the *Escherichia coli* DnaJ chaperone, J. Mol. Biol., 260 (1996) 236–250.
[157] R.B. Hill, J.M. Flanagan, J.H. Prestegard, ^{1}H and ^{15}N magnetic resonance assignments, secondary structure, and tertiary fold of *Escherichia coli* DnaJ(1-78), Biochemistry, 34 (1995) 5587–5596.
[158] Y.Q. Qian, D. Patel, F.U. Hartl, D.J. McColl, Nuclear magnetic resonance solution structure of the human Hsp40 (HDJ-1) J-domain, J. Mol. Biol., 260 (1996) 224–235.
[159] M.K. Greene, K. Maskos, S.J. Landry, Role of the J-domain in the cooperation of Hsp40 with Hsp70, Proc. Natl. Acad. Sci. USA, 95 (1998) 6108–6113.
[160] J. Wild, E. Altman, T. Yura, C.A. Gross, DnaK and DnaJ heat shock proteins participate in protein export in *Escherichia coli*, Genes Dev., 6 (1992) 1165–1172.
[161] B.E. Horne, T. Li, P. Genevaux, C. Georgopoulos, S.J. Landry, The Hsp40 J-domain stimulates Hsp70 when tethered by the client to the ATPase domain, J. Biol. Chem., 285 (2010) 21679–21688.
[162] A. Ahmad, A. Bhattacharya, R.A. McDonald, M. Cordes, B. Ellington, E.B. Bertelsen, E.R. Zuiderweg, Heat shock protein 70 kDa chaperone/DnaJ cochaperone complex employs an unusual dynamic interface, Proc. Natl. Acad. Sci. USA, 108 (2011) 18966–18971.

[163] C.J. Harrison, M. Hayer-Hartl, M. Di Liberto, F. Hartl, J. Kuriyan, Crystal structure of the nucleotide exchange factor GrpE bound to the ATPase domain of the molecular chaperone DnaK, Science, 276 (1997) 431–435.
[164] A. Nakamura, K. Takumi, K. Miki, Crystal structure of a thermophilic GrpE protein: insight into thermosensing function for the DnaK chaperone system, J. Mol. Biol., 396 (2010) 1000–1011.
[165] C.C. Wu, V. Naveen, C.H. Chien, Y.W. Chang, C.D. Hsiao, Crystal structure of DnaK protein complexed with nucleotide exchange factor GrpE in DnaK chaperone system: insight into intermolecular communication, J. Biol. Chem., 287 (2012) 21461–21470.
[166] E.A. Nollen, J.F. Brunsting, J. Song, H.H. Kampinga, R.I. Morimoto, Bag1 functions *in vivo* as a negative regulator of Hsp70 chaperone activity, Mol. Cell. Biol., 20 (2000) 1083–1088.
[167] K. Briknarova, S. Takayama, L. Brive, M.L. Havert, D.A. Knee, J. Velasco, S. Homma, E. Cabezas, J. Stuart, D.W. Hoyt, A.C. Satterthwait, M. Llinas, J.C. Reed, K.R. Ely, Structural analysis of BAG1 cochaperone and its interactions with Hsc70 heat shock protein, Nat. Struct. Biol., 8 (2001) 349–352.
[168] K. Briknarova, S. Takayama, S. Homma, K. Baker, E. Cabezas, D.W. Hoyt, Z. Li, A.C. Satterthwait, K.R. Ely, BAG4/SODD protein contains a short BAG domain, J. Biol. Chem., 277 (2002) 31172–31178.
[169] C. Brockmann, D. Leitner, D. Labudde, A. Diehl, V. Sievert, K. Büssow, R. Kühne, H. Oschkinat, The solution structure of the SODD BAG domain reveals additional electrostatic interactions in the HSP70 complexes of SODD subfamily BAG domains, FEBS Lett., 558 (2004) 101–106.
[170] K. Richter, M. Haslbeck, J. Buchner, The heat shock response: life on the verge of death, Mol. Cell, 40 (2010) 253–266.
[171] R. Zhao, M. Davey, Y.C. Hsu, P. Kaplanek, A. Tong, A.B. Parsons, N. Krogan, G. Cagney, D. Mai, J. Greenblatt, C. Boone, A. Emili, W.A. Houry, Navigating the chaperone network: an integrative map of physical and genetic interactions mediated by the Hsp90 chaperone, Cell, 120 (2005) 715–727.
[172] M. Taipale, D.F. Jarosz, S. Lindquist, HSP90 at the hub of protein homeostasis: emerging mechanistic insights, Nat. Rev. Mol. Cell Biol., 11 (2010) 515–528.
[173] J.C. Young, I. Moarefi, F.U. Hartl, Hsp90: a specialized but essential protein-folding tool, J. Cell Biol., 154 (2001) 267–273.
[174] D. Picard, Heat-shock protein 90, a chaperone for folding and regulation, Cell. Mol. Life Sci., 59 (2002) 1640–1648.
[175] A.J. McClellan, Y. Xia, A.M. Deutschbauer, R.W. Davis, M. Gerstein, J. Frydman, Diverse cellular functions of the Hsp90 molecular chaperone uncovered using systems approaches, Cell, 131 (2007) 121–135.
[176] P. Müller, P. Ceskova, B. Vojtesek, Hsp90 is essential for restoring cellular functions of temperature-sensitive p53 mutant protein but not for stabilization and activation of wild-type p53: implications for cancer therapy, J. Biol. Chem., 280 (2005) 6682–6691.
[177] C. Prodromou, S.M. Roe, R. O'Brien, J.E. Ladbury, P.W. Piper, L.H. Pearl, Identification and structural characterization of the ATP/ADP-binding site in the Hsp90 molecular chaperone, Cell, 90 (1997) 65–75.
[178] L.H. Pearl, C. Prodromou, Structure and mechanism of the Hsp90 molecular chaperone machinery, Annu. Rev. Biochem., 75 (2006) 271–294.

[179] T. Scheibel, T. Weikl, J. Buchner, Two chaperone sites in Hsp90 differing in substrate specificity and ATP dependence, Proc. Natl. Acad. Sci. USA, 95 (1998) 1495–1499.
[180] T.O. Street, L.A. Lavery, D.A. Agard, Substrate binding drives large-scale conformational changes in the Hsp90 molecular chaperone, Mol. Cell, 42 (2011) 96–105.
[181] O.R. Lorenz, L. Freiburger, D.A. Rutz, M. Krause, B.K. Zierer, S. Alvira, J. Cuellar, J.M. Valpuesta, T. Madl, M. Sattler, J. Buchner, Modulation of the Hsp90 chaperone cycle by a stringent client protein, Mol. Cell, 53 (2014) 941–953.
[182] M.M. Ali, S.M. Roe, C.K. Vaughan, P. Meyer, B. Panaretou, P.W. Piper, C. Prodromou, L.H. Pearl, Crystal structure of an Hsp90-nucleotide-p23/Sba1 closed chaperone complex, Nature, 440 (2006) 1013–1017.
[183] A.K. Shiau, S.F. Harris, D.R. Southworth, D.A. Agard, Structural Analysis of *E. coli* Hsp90 reveals dramatic nucleotide-dependent conformational rearrangements, Cell, 127 (2006) 329–340.
[184] R.M. Salek, M.A. Williams, C. Prodromou, L.H. Pearl, J.E. Ladbury, Backbone resonance assignments of the 25kD N-terminal ATPase domain from the Hsp90 chaperone, J. Biomol. NMR, 23 (2002) 327–328.
[185] D.M. Jacobs, T. Langer, B. Elshorst, K. Saxena, K.M. Fiebig, M. Vogtherr, H. Schwalbe, NMR backbone assignment of the N-terminal domain of human HSP90, J. Biomol. NMR, 36 (2006) 52.
[186] R. Riek, G. Wider, K. Pervushin, K. Wüthrich, Polarization transfer by cross-correlated relaxation in solution NMR with very large molecules, Proc. Natl. Acad. Sci. USA, 96 (1999) 4918–4923.
[187] S. Rüdiger, S.M.V. Freund, D.B. Veprintsev, A.R. Fersht, CRINEPT-TROSY NMR reveals p53 core domain bound in an unfolded form to the chaperone Hsp90, Proc. Natl. Acad. Sci. USA, 99 (2002) 11085–11090.
[188] S.J. Park, B.N. Borin, M.A. Martinez-Yamout, H.J. Dyson, The client protein p53 adopts a molten globule-like state in the presence of Hsp90, Nat. Struct. Mol. Biol., 18 (2011) 537–541.
[189] S.J. Park, M. Kostic, H.J. Dyson, Dynamic interaction of Hsp90 with its client protein p53, J. Mol. Biol., 411 (2011) 158–173.
[190] T. Didenko, A.M. Duarte, G.E. Karagöz, S.G. Rüdiger, Hsp90 structure and function studied by NMR spectroscopy, Biochim. Biophys. Acta, 1823 (2012) 636-647.
[191] T.O. Street, X. Zeng, R. Pellarin, M. Bonomi, A. Šali, M.J. Kelly, F. Chu, D.A. Agard, Elucidating the mechanism of substrate recognition by the bacterial Hsp90 molecular chaperone, J. Mol. Biol., 426 (2014) 2393–2404.
[192] G.E. Karagöz, A.M. Duarte, E. Akoury, H. Ippel, J. Biernat, T. Moran Luengo, M. Radli, T. Didenko, B.A. Nordhues, D.B. Veprintsev, C.A. Dickey, E. Mandelkow, M. Zweckstetter, R. Boelens, T. Madl, S.G. Rüdiger, Hsp90-Tau complex reveals molecular basis for specificity in chaperone action, Cell, 156 (2014) 963–974.
[193] M.A. Martinez-Yamout, R.P. Venkitakrishnan, N.E. Preece, G. Kroon, P.E. Wright, H.J. Dyson, Localization of sites of interaction between p23 and Hsp90 in solution, J. Biol. Chem., 281 (2006) 14457–14464.
[194] G.E. Karagöz, A.M. Duarte, H. Ippel, C. Uetrecht, T. Sinnige, M. van Rosmalen, J. Hausmann, A.J. Heck, R. Boelens, S.G. Rüdiger, N-terminal domain of human Hsp90 triggers binding to the cochaperone p23, Proc. Natl. Acad. Sci. USA, 108 (2011) 580–585.
[195] M. Retzlaff, F. Hagn, L. Mitschke, M. Hessling, F. Gugel, H. Kessler, K. Richter, J. Buchner, Asymmetric activation of the Hsp90 dimer by its cochaperone Aha1, Mol. Cell, 37 (2010) 344–354.

[196] J. Li, K. Richter, J. Reinstein, J. Buchner, Integration of the accelerator Aha1 in the Hsp90 co-chaperone cycle, Nat. Struct. Mol. Biol., 20 (2013) 326–331.
[197] S. Sreeramulu, H.R. Jonker, T. Langer, C. Richter, C.R. Lancaster, H. Schwalbe, The human Cdc37.Hsp90 complex studied by heteronuclear NMR spectroscopy, J. Biol. Chem., 284 (2009) 3885–3896.
[198] Y.T. Lee, J. Jacob, W. Michowski, M. Nowotny, J. Kuznicki, W.J. Chazin, Human Sgt1 binds HSP90 through the CHORD-Sgt1 domain and not the tetratricopeptide repeat domain, J. Biol. Chem., 279 (2004) 16511–16517.
[199] M. Linnert, Y.J. Lin, A. Manns, K. Haupt, A.K. Paschke, G. Fischer, M. Weiwad, C. Lücke, The FKBP-type domain of the human aryl hydrocarbon receptor-interacting protein reveals an unusual Hsp90 interaction, Biochemistry, 52 (2013) 2097–2107.
[200] S. Boulon, B. Pradet-Balade, C. Verheggen, D. Molle, S. Boireau, M. Georgieva, K. Azzag, M.C. Robert, Y. Ahmad, H. Neel, A.I. Lamond, E. Bertrand, HSP90 and its R2TP/Prefoldin-like cochaperone are involved in the cytoplasmic assembly of RNA polymerase II, Mol. Cell, 39 (2010) 912–924.
[201] L. Ni, M. Saeki, L. Xu, H. Nakahara, M. Saijo, K. Tanaka, Y. Kamisaki, RPAP3 interacts with Reptin to regulate UV-induced phosphorylation of H2AX and DNA damage, J Cell Biochem, 106 (2009) 920–928.
[202] B. Jimenez, F. Ugwu, R. Zhao, L. Orti, T. Makhnevych, A. Pineda-Lucena, W.A. Houry, Structure of minimal tetratricopeptide repeat domain protein Tah1 reveals mechanism of its interaction with Pih1 and Hsp90, J. Biol. Chem., 287 (2012) 5698–5709.
[203] R. Back, C. Dominguez, B. Rothe, C. Bobo, C. Beaufils, S. Morera, P. Meyer, B. Charpentier, C. Branlant, F.H. Allain, X. Manival, High-resolution structural analysis shows how Tah1 tethers Hsp90 to the R2TP complex, Structure, 21 (2013) 1834–1847.
[204] A. Dehner, J. Furrer, K. Richter, I. Schuster, J. Buchner, H. Kessler, NMR chemical shift perturbation study of the N-terminal domain of Hsp90 upon binding of ADP, AMP-PNP, geldanamycin, and radicicol, Chembiochem, 4 (2003) 870–877.
[205] B.K. Zierer, M. Weiwad, M. Rubbelke, L. Freiburger, G. Fischer, O.R. Lorenz, M. Sattler, K. Richter, J. Buchner, Artificial accelerators of the molecular chaperone Hsp90 facilitate rate-limiting conformational transitions, Angew. Chem. Int. Ed. Engl., (2014) in press.
[206] H.R. Saibil, W.A. Fenton, D.K. Clare, A.L. Horwich, Structure and allostery of the chaperonin GroEL, J. Mol. Biol., 425 (2013) 1476–1487.
[207] S.J. Landry, L.M. Gierasch, The chaperonin GroEL binds a polypeptide in an α-helical conformation, Biochemistry, 30 (1991) 7359–7362.
[208] Z. Wang, H. Feng, S.J. Landry, J. Maxwell, L.M. Gierasch, Basis of substrate binding by the chaperonin GroEL, Biochemistry, 38 (1999) 12537–12546.
[209] R. Zahn, S. Perrett, G. Stenberg, A.R. Fersht, Catalysis of amide proton exchange by the molecular chaperones GroEL and SecB, Science, 271 (1996) 642–645.
[210] S.E. Nieba-Axmann, M. Ottiger, K. Wüthrich, A. Plückthun, Multiple cycles of global unfolding of GroEL-bound cyclophilin A evidenced by NMR, J. Mol. Biol., 271 (1997) 803–818.
[211] S.J. Landry, J. Zeilstra-Ryalls, O. Fayet, C. Georgopoulos, L.M. Gierasch, Characterization of a functionally important mobile domain of GroES, Nature, 364 (1993) 255–258.
[212] F. Shewmaker, K. Maskos, C. Simmerling, S.J. Landry, The disordered mobile loop of GroES folds into a defined β-hairpin upon binding GroEL, J. Biol. Chem., 276 (2001) 31257–31264.

[213] M.K. Hayer-Hartl, F. Weber, F.U. Hartl, Mechanism of chaperonin action: GroES binding and release can drive GroEL-mediated protein folding in the absence of ATP hydrolysis, EMBO J., 15 (1996) 6111–6121.
[214] A.M. Buckle, R. Zahn, A.R. Fersht, A structural model for GroEL-polypeptide recognition, Proc. Natl. Acad. Sci. USA, 94 (1997) 3571–3575.
[215] L. Chen, P.B. Sigler, The crystal structure of a GroEL/peptide complex: plasticity as a basis for substrate diversity, Cell, 99 (1999) 757–768.
[216] Q. Hua, I.S. Dementieva, M.A. Walsh, K. Hallenga, M.A. Weiss, A. Joachimiak, A thermophilic mini-chaperonin contains a conserved polypeptide-binding surface: combined crystallographic and NMR studies of the GroEL apical domain with implications for substrate interactions, J. Mol. Biol., 306 (2001) 513–525.
[217] Y. Li, X. Gao, L. Chen, GroEL recognizes an amphipathic helix and binds to the hydrophobic side, J. Biol. Chem., 284 (2009) 4324–4331.
[218] M. Gozu, M. Hoshino, T. Higurashi, H. Kato, Y. Goto, The interaction of β_2-glycoprotein I domain V with chaperonin GroEL: the similarity with the domain V and membrane interaction, Protein Sci., 11 (2002) 2792–2803.
[219] N. Kobayashi, S.M. Freund, J. Chatellier, R. Zahn, A.R. Fersht, NMR analysis of the binding of a rhodanese peptide to a minichaperone in solution, J. Mol. Biol., 292 (1999) 181–190.
[220] N.A. Ranson, D.K. Clare, G.W. Farr, D. Houldershaw, A.L. Horwich, H.R. Saibil, Allosteric signaling of ATP hydrolysis in GroEL-GroES complexes, Nat. Struct. Mol. Biol., 13 (2006) 147–352.
[221] K. Pervushin, R. Riek, G. Wider, K. Wüthrich, Attenuated T_2 relaxation by mutual cancellation of dipole-dipole coupling and chemical shift anisotropy indicates an avenue to NMR structures of very large biological macromolecules in solution, Proc. Natl. Acad. Sci. USA, 94 (1997) 12366–12371.
[222] J. Fiaux, E.B. Bertelsen, A.L. Horwich, K. Wüthrich, NMR analysis of a 900K GroEL GroES complex, Nature, 418 (2002) 207–211.
[223] N. Nishida, F. Motojima, M. Idota, H. Fujikawa, M. Yoshida, I. Shimada, K. Kato, Probing dynamics and conformational change of the GroEL-GroES complex by ^{13}C NMR spectroscopy, J. Biochem., 140 (2006) 591–598.
[224] R. Horst, E.B. Bertelsen, J. Fiaux, G. Wider, A.L. Horwich, K. Wüthrich, Direct NMR observation of a substrate protein bound to the chaperonin GroEL, Proc. Natl. Acad. Sci. USA, 102 (2005) 12748–12753.
[225] E. Koculi, R. Horst, A.L. Horwich, K. Wüthrich, Nuclear magnetic resonance spectroscopy with the stringent substrate rhodanese bound to the single-ring variant SR1 of the *E. coli* chaperonin GroEL, Protein Sci., 20 (2011) 1380–1386.
[226] N. Nishida, M. Yagi-Utsumi, F. Motojima, M. Yoshida, I. Shimada, K. Kato, Nuclear magnetic resonance approaches for characterizing interactions between the bacterial chaperonin GroEL and unstructured proteins, J. Biosci. Bioeng., 116 (2013) 160–164.
[227] M. Yagi-Utsumi, T. Kunihara, T. Nakamura, Y. Uekusa, K. Makabe, K. Kuwajima, K. Kato, NMR characterization of the interaction of GroEL with amyloid β as a model ligand, FEBS Lett., 587 (2013) 1605–1609.
[228] D.A. Dougan, A. Mogk, K. Zeth, K. Turgay, B. Bukau, AAA+ proteins and substrate recognition, it all depends on their partner in crime, FEBS Lett., 529 (2002) 6–10.
[229] L.W. Donaldson, U. Wojtyra, W.A. Houry, Solution structure of the dimeric zinc binding domain of the chaperone ClpX, J. Biol. Chem., 278 (2003) 48991–48996.
[230] N.V. Grishin, Treble clef finger––a functionally diverse zinc-binding structural motif, Nucleic Acids Res., 29 (2001) 1703–1714.

[231] D.J. Kojetin, P.D. McLaughlin, R.J. Thompson, D. Dubnau, P. Prepiak, M. Rance, J. Cavanagh, Structural and motional contributions of the *Bacillus subtilis* ClpC N-domain to adaptor protein interactions, J. Mol. Biol., 387 (2009) 639–652.
[232] D.J. Kojetin, P.D. McLaughlin, R.J. Thompson, R.A. Venters, M. Rance, J. Cavanagh, NMR assignment of the N-terminal repeat domain of *Bacillus subtilis* ClpC, Biomol. NMR Assign., 1 (2007) 163–165.
[233] G. Thibault, J. Yudin, P. Wong, V. Tsitrin, R. Sprangers, R. Zhao, W.A. Houry, Specificity in substrate and cofactor recognition by the N-terminal domain of the chaperone ClpX, Proc. Natl. Acad. Sci. USA, 103 (2006) 17724–17729.
[234] I. Levchenko, M. Seidel, R.T. Sauer, T.A. Baker, A specificity-enhancing factor for the ClpXP degradation machine, Science, 289 (2000) 2354–2356.
[235] G. Thibault, W.A. Houry, Role of the N-terminal domain of the chaperone ClpX in the recognition and degradation of λ phage protein O, J. Phys. Chem. B, 116 (2012) 6717–6724.
[236] R. Sprangers, A. Gribun, P.M. Hwang, W.A. Houry, L.E. Kay, Quantitative NMR spectroscopy of supramolecular complexes: dynamic side pores in ClpP are important for product release, Proc. Natl. Acad. Sci. USA, 102 (2005) 16678–16683.
[237] T.L. Religa, A.M. Ruschak, R. Rosenzweig, L.E. Kay, Site-directed methyl group labeling as an NMR probe of structure and dynamics in supramolecular protein systems: applications to the proteasome and to the ClpP protease, J. Am. Chem. Soc., 133 (2011) 9063–9068.
[238] M.C. Bewley, V. Graziano, K. Griffin, J.M. Flanagan, The asymmetry in the mature amino-terminus of ClpP facilitates a local symmetry match in ClpAP and ClpXP complexes, J. Struct. Biol., 153 (2006) 113–128.
[239] H.R. Saibil, Biochemistry. Machinery to reverse irreversible aggregates, Science, 339 (2013) 1040–1041.
[240] M. Groll, L. Ditzel, J. Löwe, D. Stock, M. Bochtler, H.D. Bartunik, R. Huber, Structure of 20S proteasome from yeast at 2.4 Å resolution, Nature, 386 (1997) 463–471.
[241] E. Seemüller, A. Lupas, D. Stock, J. Löwe, R. Huber, W. Baumeister, Proteasome from *Thermoplasma acidophilum*: a threonine protease, Science, 268 (1995) 579–582.
[242] M. Unno, T. Mizushima, Y. Morimoto, Y. Tomisugi, K. Tanaka, N. Yasuoka, T. Tsukihara, The structure of the mammalian 20S proteasome at 2.75 Å resolution, Structure, 10 (2002) 609–618.
[243] E. Kish-Trier, C.P. Hill, Structural biology of the proteasome, Annu. Rev. Biophys., 42 (2013) 29–49.
[244] R. Sprangers, L.E. Kay, Quantitative dynamics and binding studies of the 20S proteasome by NMR, Nature, 445 (2007) 618–622.
[245] T.L. Religa, R. Sprangers, L.E. Kay, Dynamic regulation of archaeal proteasome gate opening as studied by TROSY NMR, Science, 328 (2010) 98–102.
[246] V. Tugarinov, R. Sprangers, L.E. Kay, Probing side-chain dynamics in the proteasome by relaxation violated coherence transfer NMR spectroscopy, J. Am. Chem. Soc., 129 (2007) 1743–1750.
[247] M.P. Latham, A. Sekhar, L.E. Kay, Understanding the mechanism of proteasome 20S core particle gating, Proc. Natl. Acad. Sci. USA, 111 (2014) 5532–5537.
[248] A.M. Ruschak, L.E. Kay, Proteasome allostery as a population shift between interchanging conformers, Proc. Natl. Acad. Sci. USA, 109 (2012) 3454–3462.
[249] L. Shi, L.E. Kay, Tracing an allosteric pathway regulating the activity of the HslV protease, Proc. Natl. Acad. Sci. USA, 111 (2014) 2140–2145.

[250] A.M. Ruschak, T.L. Religa, S. Breuer, S. Witt, L.E. Kay, The proteasome antechamber maintains substrates in an unfolded state, Nature, 467 (2010) 868–871.
[251] R. Sprangers, X. Li, X. Mao, J.L. Rubinstein, A.D. Schimmer, L.E. Kay, TROSY-based NMR evidence for a novel class of 20S proteasome inhibitors, Biochemistry, 47 (2008) 6727–6734.
[252] M. Keita, J. Kaffy, C. Troufflard, E. Morvan, B. Crousse, S. Ongeri, ^{19}F NMR monitoring of the eukaryotic 20S proteasome chymotrypsin-like activity: an investigative tool for studying allosteric regulation, Org. Biomol. Chem., 12 (2014) 4576–4581.
[253] A. Velyvis, L.E. Kay, Measurement of active site ionization equilibria in the 670 kDa proteasome core particle using methyl-TROSY NMR, J. Am. Chem. Soc., 135 (2013) 9259–9262.
[254] M. Musial-Siwek, S.L. Rusch, D.A. Kendall, Selective photoaffinity labeling identifies the signal peptide binding domain on SecA, J. Mol. Biol., 365 (2007) 637–648.
[255] K. Mitra, J. Frank, A. Driessen, Co- and post-translational translocation through the protein-conducting channel: analogous mechanisms at work?, Nat. Struct. Mol. Biol., 13 (2006) 957–964.
[256] E. Vrontou, A. Economou, Structure and function of SecA, the preprotein translocase nanomotor, Biochim. Biophys. Acta, 1694 (2004) 67–80.
[257] T.L. Volkert, J.D. Baleja, C.A. Kumamoto, A highly mobile C-terminal tail of the *Escherichia coli* protein export chaperone SecB, Biochem. Biophys. Res. Commun., 264 (1999) 949–954.
[258] W.M. Matousek, A.T. Alexandrescu, NMR structure of the C-terminal domain of SecA in the free state, Biochim. Biophys. Acta, 1702 (2004) 163–171.
[259] B.R. Dempsey, M. Wrona, J.M. Moulin, G.B. Gloor, F. Jalilehvand, G. Lajoie, G.S. Shaw, B.H. Shilton, Solution NMR structure and X-ray absorption analysis of the C-terminal zinc-binding domain of the SecA ATPase, Biochemistry, 43 (2004) 9361–9371.
[260] I. Gelis, A.M. Bonvin, D. Keramisanou, M. Koukaki, G. Gouridis, S. Karamanou, A. Economou, C.G. Kalodimos, Structural basis for signal-sequence recognition by the translocase motor SecA as determined by NMR, Cell, 131 (2007) 756–769.
[261] G. Sianidis, S. Karamanou, E. Vrontou, K. Boulias, K. Repanas, N. Kyrpides, A.S. Politou, A. Economou, Cross-talk between catalytic and regulatory elements in a DEAD motor domain is essential for SecA function, EMBO J., 20 (2001) 961–970.
[262] Y.T. Chou, J.F. Swain, L.M. Gierasch, Functionally significant mobile regions of *Escherichia coli* SecA ATPase identified by NMR, J. Biol. Chem., 277 (2002) 50985–50990.
[263] D. Keramisanou, N. Biris, I. Gelis, G. Sianidis, S. Karamanou, A. Economou, C.G. Kalodimos, Disorder-order folding transitions underlie catalysis in the helicase motor of SecA, Nat. Struct. Mol. Biol., 13 (2006) 594–602.
[264] J.F. Hunt, S. Weinkauf, L. Henry, J.J. Fak, P. McNicholas, D.B. Oliver, J. Deisenhofer, Nucleotide control of interdomain interactions in the conformational reaction cycle of SecA, Science, 297 (2002) 2018–2026.
[265] Y.T. Chou, L.M. Gierasch, The conformation of a signal peptide bound by *Escherichia coli* preprotein translocase SecA, J. Biol. Chem., 280 (2005) 32753–32760.
[266] E. Papanikou, S. Karamanou, C. Baud, M. Frank, G. Sianidis, D. Keramisanou, C.G. Kalodimos, A. Kuhn, A. Economou, Identification of the preprotein binding domain of SecA, J. Biol. Chem., 280 (2005) 43209–43217.

[267] S. Karamanou, G. Gouridis, E. Papanikou, G. Sianidis, I. Gelis, D. Keramisanou, E. Vrontou, C.G. Kalodimos, A. Economou, Preprotein-controlled catalysis in the helicase motor of SecA, EMBO J., 26 (2007) 2904–2914.
[268] S.M. Doyle, E.H. Braswell, C.M. Teschke, SecA folds *via* a dimeric intermediate, Biochemistry, 39 (2000) 11667–11676.
[269] L. Reggie, J.J. Lopez, I. Collinson, C. Glaubitz, M. Lorch, Dynamic nuclear polarization-enhanced solid-state NMR of a ^{13}C-labeled signal peptide bound to lipid-reconstituted Sec translocon, J. Am. Chem. Soc., 133 (2011) 19084–19086.
[270] N. Ruiz, D. Kahne, T.J. Silhavy, Advances in understanding bacterial outer-membrane biogenesis, Nat. Rev. Microbiol., 4 (2006) 57–66.
[271] J.G. Sklar, T. Wu, D. Kahne, T.J. Silhavy, Defining the roles of the periplasmic chaperones SurA, Skp, and DegP in *Escherichia coli*, Gene Dev., 21 (2007) 2473–2484.
[272] E. Bitto, D.B. McKay, Crystallographic structure of SurA, a molecular chaperone that facilitates folding of outer membrane porins, Structure, 10 (2002) 1489–1498.
[273] X. Xu, S. Wang, Y.X. Hu, D.B. McKay, The periplasmic bacterial molecular chaperone SurA adapts its structure to bind peptides in different conformations to assert a sequence preference for aromatic residues, J. Mol. Biol., 373 (2007) 367–381.
[274] T.A. Walton, M.C. Sousa, Crystal structure of Skp, a prefoldin-like chaperone that protects soluble and membrane proteins from aggregation, Mol. Cell, 15 (2004) 367–374.
[275] I.P. Korndörfer, M.K. Dommel, A. Skerra, Structure of the periplasmic chaperone Skp suggests functional similarity with cytosolic chaperones despite differing architecture, Nat. Struct. Mol. Biol., 11 (2004) 1015–1020.
[276] J. Qu, C. Mayer, S. Behrens, O. Holst, J.H. Kleinschmidt, The trimeric periplasmic chaperone Skp of *Escherichia coli* forms 1:1 complexes with outer membrane proteins *via* hydrophobic and electrostatic interactions, J. Mol. Biol., 374 (2007) 91–105.
[277] T.A. Walton, C.M. Sandoval, C.A. Fowler, A. Pardi, M.C. Sousa, The cavity-chaperone Skp protects its substrate from aggregation but allows independent folding of substrate domains, Proc. Natl. Acad. Sci. USA, 106 (2009) 1772–1777.
[278] B.M. Burmann, S. Hiller, Solution NMR Studies of Membrane-Protein-Chaperone Complexes, Chimia, 66 (2012) 759–763.
[279] K. Hu, A. Plückthun, K. Pervushin, Backbone H^N, N, C^α, C' and C^β chemical shift assignments and secondary structure of FkpA, a 245-residue peptidyl-prolyl cis/trans isomerase with chaperone activity, J. Biomol. NMR, 28 (2004) 405–406.
[280] K. Hu, V. Galius, K. Pervushin, Structural plasticity of peptidyl-prolyl isomerase sFkpA is a key to its chaperone function as revealed by solution NMR, Biochemistry, 45 (2006) 11983–11991.
[281] F.A. Saul, J.P. Arie, B. Vulliez-le Normand, R. Kahn, J.M. Betton, G.A. Bentley, Structural and functional studies of FkpA from *Escherichia coli*, a cis/trans peptidyl-prolyl isomerase with chaperone activity, J. Mol. Biol., 335 (2004) 595–608.
[282] C. Dartigalongue, S. Raina, A new heat-shock gene, *ppiD*, encodes a peptidyl-prolyl isomerase required for folding of outer membrane proteins in *Escherichia coli*, EMBO J., 17 (1998) 3968–3980.
[283] U. Weininger, R.P. Jakob, M. Kovermann, J. Balbach, F.X. Schmid, The prolyl isomerase domain of PpiD from *Escherichia coli* shows a parvulin fold but is devoid of catalytic activity, Protein Sci., 19 (2010) 6–18.
[284] M. Haslbeck, T. Franzmann, D. Weinfurtner, J. Buchner, Some like it hot: the structure and function of small heat-shock proteins, Nat. Struct. Mol. Biol., 12 (2005) 842–846.

[285] H. Ecroyd, J.A. Carver, Crystallin proteins and amyloid fibrils, Cell. Mol. Life Sci., 66 (2009) 62–81.
[286] J. Horwitz, α-crystallin can function as a molecular chaperone, Proc. Natl. Acad. Sci. USA, 89 (1992) 10449–10453.
[287] D.I. Lin, O. Barbash, K.G. Kumar, J.D. Weber, J.W. Harper, A.J. Klein-Szanto, A. Rustgi, S.Y. Fuchs, J.A. Diehl, Phosphorylation-dependent ubiquitination of cyclin D1 by the SCF(FBX4–αB crystallin) complex, Mol. Cell, 24 (2006) 355–366.
[288] D. Selcen, A.G. Engel, Myofibrillar myopathy caused by novel dominant negative αB-crystallin mutations, Ann. Neurol., 54 (2003) 804–810.
[289] L.E. Goldstein, J.A. Muffat, R.A. Cherny, R.D. Moir, M.H. Ericsson, X. Huang, C. Mavros, J.A. Coccia, K.Y. Faget, K.A. Fitch, C.L. Masters, R.E. Tanzi, L.T. Chylack, Jr., A.I. Bush, Cytosolic β-amyloid deposition and supranuclear cataracts in lenses from people with Alzheimer's disease, Lancet, 361 (2003) 1258–1265.
[290] K. Kato, Y. Inaguma, H. Ito, K. Iida, I. Iwamoto, K. Kamei, N. Ochi, H. Ohta, M. Kishikawa, Ser-59 is the major phosphorylation site in αB-crystallin accumulated in the brains of patients with Alexander's disease, J. Neurochem., 76 (2001) 730–736.
[291] P. Vicart, A. Caron, P. Guicheney, Z. Li, M.C. Prevost, A. Faure, D. Chateau, F. Chapon, F. Tome, J.M. Dupret, D. Paulin, M. Fardeau, A missense mutation in the αB-crystallin chaperone gene causes a desmin-related myopathy, Nat. Genet., 20 (1998) 92–95.
[292] N.S. Rajasekaran, P. Connell, E.S. Christians, L.J. Yan, R.P. Taylor, A. Orosz, X.Q. Zhang, T.J. Stevenson, R.M. Peshock, J.A. Leopold, W.H. Barry, J. Loscalzo, S.J. Odelberg, I.J. Benjamin, Human αB-crystallin mutation causes oxido-reductive stress and protein aggregation cardiomyopathy in mice, Cell, 130 (2007) 427–439.
[293] J.A. Aquilina, J.L. Benesch, O.A. Bateman, C. Slingsby, C.V. Robinson, Polydispersity of a mammalian chaperone: mass spectrometry reveals the population of oligomers in αB-crystallin, Proc. Natl. Acad. Sci. USA, 100 (2003) 10611–10616.
[294] P.J. Werten, J.A. Carver, R. Jaenicke, W.W. de Jong, The elusive role of the N-terminal extension of βA3- and βA1-crystallin, Protein Eng., 9 (1996) 1021–1028.
[295] J.A. Carver, J.A. Aquilina, R.J. Truscott, G.B. Ralston, Identification by ^{1}H NMR spectroscopy of flexible C-terminal extensions in bovine lens α-crystallin, FEBS Lett., 311 (1992) 143–149.
[296] J.A. Carver, G. Esposito, G. Schwedersky, M. Gaestel, ^{1}H NMR spectroscopy reveals that mouse Hsp25 has a flexible C-terminal extension of 18 amino acids, FEBS Lett., 369 (1995) 305–310.
[297] F.A. van de Klundert, R.H. Smulders, M.L. Gijsen, R.A. Lindner, R. Jaenicke, J.A. Carver, W.W. de Jong, The mammalian small heat-shock protein Hsp20 forms dimers and is a poor chaperone, Eur. J. Biochem., 258 (1998) 1014–1021.
[298] R.A. Lindner, J.A. Carver, M. Ehrnsperger, J. Buchner, G. Esposito, J. Behlke, G. Lutsch, A. Kotlyarov, M. Gaestel, Mouse Hsp25, a small shock protein. The role of its C-terminal extension in oligomerization and chaperone action, Eur. J. Biochem., 267 (2000) 1923–1932.
[299] R.H.P.H. Smulders, J.A. Carver, R.A. Lindner, M.A. van Boekel, H. Bloemendal, W.W. de Jong, Immobilization of the C-terminal extension of bovine αA-crystallin reduces chaperone-like activity, J. Biol. Chem., 271 (1996) 29060–29066.
[300] T.M. Treweek, A. Rekas, M.J. Walker, J.A. Carver, A quantitative NMR spectroscopic examination of the flexibility of the C-terminal extensions of the molecular chaperones, αA- and αB-crystallin, Exp. Eye Res., 91 (2010) 691–699.

[301] S. Narayanan, B. Kamps, W.C. Boelens, B. Reif, αB-crystallin competes with Alzheimer's disease β-amyloid peptide for peptide-peptide interactions and induces oxidation of Aβ-Met35, FEBS Lett., 580 (2006) 5941–5946.
[302] J.J. Liang, Interaction between β-amyloid and lens αB-crystallin, FEBS Lett., 484 (2000) 98–101.
[303] J. Kanski, S. Varadarajan, M. Aksenova, D.A. Butterfield, Role of glycine-33 and methionine-35 in Alzheimer's amyloid β-peptide 1-42-associated oxidative stress and neurotoxicity, Biochim. Biophys. Acta, 1586 (2002) 190–198.
[304] A.J. Baldwin, G.R. Hilton, H. Lioe, C. Bagneris, J.L. Benesch, L.E. Kay, Quaternary dynamics of αB-crystallin as a direct consequence of localised tertiary fluctuations in the C-terminus, J. Mol. Biol., 413 (2011) 310–320.
[305] A.J. Baldwin, H. Lioe, C.V. Robinson, L.E. Kay, J.L. Benesch, αB-crystallin polydispersity is a consequence of unbiased quaternary dynamics, J. Mol. Biol., 413 (2011) 297–309.
[306] S. Jehle, B. van Rossum, J.R. Stout, S.M. Noguchi, K. Falber, K. Rehbein, H. Oschkinat, R.E. Klevit, P. Rajagopal, αB-crystallin: a hybrid solid-state/solution-state NMR investigation reveals structural aspects of the heterogeneous oligomer, J. Mol. Biol., 385 (2009) 1481–1497.
[307] J. Peschek, N. Braun, T.M. Franzmann, Y. Georgalis, M. Haslbeck, S. Weinkauf, J. Buchner, The eye lens chaperone αB-crystallin forms defined globular assemblies, Proc. Natl. Acad. Sci. USA, 106 (2009) 13272–13277.
[308] S. Jehle, B.S. Vollmar, B. Bardiaux, K.K. Dove, P. Rajagopal, T. Gonen, H. Oschkinat, R.E. Klevit, N-terminal domain of αB-crystallin provides a conformational switch for multimerization and structural heterogeneity, Proc. Natl. Acad. Sci. USA, 108 (2011) 6409–6414.
[309] S.P. Delbecq, S. Jehle, R. Klevit, Binding determinants of the small heat shock protein, αB-crystallin: recognition of the 'IxI' motif, EMBO J., 31 (2012) 4587–4594.
[310] A.J. Baldwin, L.E. Kay, Measurement of the signs of methyl ^{13}C chemical shift differences between interconverting ground and excited protein states by $R_{1\rho}$: an application to αB-crystallin, J. Biomol. NMR, 53 (2012) 1–12.
[311] A.J. Baldwin, P. Walsh, D.F. Hansen, G.R. Hilton, J.L. Benesch, S. Sharpe, L.E. Kay, Probing dynamic conformations of the high-molecular-weight αB-crystallin heat shock protein ensemble by NMR spectroscopy, J. Am. Chem. Soc., 134 (2012) 15343–15350.
[312] R.A. Lindner, A. Kapur, J.A. Carver, The interaction of the molecular chaperone, αB-crystallin, with molten globule states of bovine α-lactalbumin, J. Biol. Chem., 272 (1997) 27722–27729.
[313] G. Esposito, M. Garvey, V. Alverdi, F. Pettirossi, A. Corazza, F. Fogolari, M. Polano, P.P. Mangione, S. Giorgetti, M. Stoppini, A. Rekas, V. Bellotti, A.J. Heck, J.A. Carver, Monitoring the interaction between β2-microglobulin and the molecular chaperone αB-crystallin by NMR and mass spectrometry: αB-crystallin dissociates β_2-microglobulin oligomers, J. Biol. Chem., 288 (2013) 17844–17858.
[314] C.N. Kingsley, W.D. Brubaker, S. Markovic, A. Diehl, A.J. Brindley, H. Oschkinat, R.W. Martin, Preferential and specific binding of human αB-crystallin to a cataract-related variant of γS-crystallin, Structure, 21 (2013) 2221–2227.
[315] N.W. Rigel, T.J. Silhavy, Making a β–barrel: assembly of outer membrane proteins in Gram-negative bacteria, Curr. Opin. Microbiol., 15 (2012) 189–193.
[316] R. Voulhoux, M.P. Bos, J. Geurtsen, M. Mols, J. Tommassen, Role of a highly conserved bacterial protein in outer membrane protein assembly, Science, 299 (2003) 262–265.

[317] L. Morgado, K. Zeth, B.M. Burmann, T. Maier, S. Hiller, Characterization of the insertase BamA in different membrane mimetics by solution NMR spectroscopy, (2014) in press.
[318] T. Sinnige, K. Houben, I. Pritisanac, M. Renault, R. Boelens, M. Baldus, Insight into the conformational stability of membrane-embedded BamA using a combined solution and solid-state NMR approach, J. Biomol. NMR, (2015) in press.
[319] T. Sinnige, M. Weingarth, M. Renault, L. Baker, J. Tommassen, M. Baldus, Solid-state NMR studies of full-length BamA in lipid bilayers suggest limited overall POTRA mobility, J. Mol. Biol., 426 (2014) 2009–2021.
[320] T.J. Knowles, M. Jeeves, S. Bobat, F. Dancea, D. McClelland, T. Palmer, M. Overduin, I.R. Henderson, Fold and function of polypeptide transport-associated domains responsible for delivering unfolded proteins to membranes, Mol. Microbiol., 68 (2008) 1216–1227.
[321] S. Kim, J.C. Malinverni, P. Sliz, T.J. Silhavy, S.C. Harrison, D. Kahne, Structure and function of an essential component of the outer membrane protein assembly machine, Science, 317 (2007) 961–964.
[322] P.Z. Gatzeva-Topalova, L.R. Warner, A. Pardi, M.C. Sousa, Structure and flexibility of the complete periplasmic domain of BamA: the protein insertion machine of the outer membrane, Structure, 18 (2010) 1492–1501.
[323] P. König, O. Mirus, R. Haarmann, M.S. Sommer, I. Sinning, E. Schleiff, I. Tews, Conserved properties of polypeptide transport-associated (POTRA) domains derived from cyanobacterial Omp85, J. Biol. Chem., 285 (2010) 18016–18024.
[324] M. Renault, M.P. Bos, J. Tommassen, M. Baldus, Solid-state NMR on a large multidomain integral membrane protein: the outer membrane protein assembly factor BamA, J. Am. Chem. Soc., 133 (2011) 4175–4177.
[325] L.M. McMorran, D.J. Brockwell, S.E. Radford, Mechanistic studies of the biogenesis and folding of outer membrane proteins *in vitro* and *in vivo*: What have we learned to date?, Arch. Biochem. Biophys., (2014) 265–280.
[326] T.J. Knowles, A. Scott-Tucker, M. Overduin, I.R. Henderson, Membrane protein architects: the role of the BAM complex in outer membrane protein assembly, Nat. Rev. Microbiol., 7 (2009) 206–214.
[327] I.E. Vainberg, S.A. Lewis, H. Rommelaere, C. Ampe, J. Vandekerckhove, H.L. Klein, N.J. Cowan, Prefoldin, a chaperone that delivers unfolded proteins to cytosolic chaperonin, Cell, 93 (1998) 863–873.
[328] R. Siegert, M.R. Leroux, C. Scheufler, F.U. Hartl, I. Moarefi, Structure of the molecular chaperone prefoldin: Unique interaction of multiple coiled coil tentacles with unfolded proteins, Cell, 103 (2000) 621–632.
[329] M.R. Leroux, M. Fändrich, D. Klunker, K. Siegers, A.N. Lupas, J.R. Brown, E. Schiebel, C.M. Dobson, F.U. Hartl, MtGimC, a novel archaeal chaperone related to the eukaryotic chaperonin cofactor GimC/prefoldin, EMBO J., 18 (1999) 6730–6743.
[330] E. Kurimoto, Y. Nishi, Y. Yamaguchi, T. Zako, R. Iizuka, N. Ide, M. Yohda, K. Kato, Dynamics of group II chaperonin and prefoldin probed by ^{13}C NMR spectroscopy, Proteins, 70 (2008) 1257–1263.
[331] Y.C. Tang, H.C. Chang, A. Roeben, D. Wischnewski, N. Wischnewski, M.J. Kerner, F.U. Hartl, M. Hayer-Hartl, Structural features of the GroEL-GroES nano-cage required for rapid folding of encapsulated protein, Cell, 125 (2006) 903–914.
[332] L.A. Joachimiak, T. Walzthoeni, C.W. Liu, R. Aebersold, J. Frydman, The structural basis of substrate recognition by the eukaryotic chaperonin TRiC/CCT, Cell, 159 (2014) 1042–1055.

[333] M. Vitikainen, I. Lappalainen, R. Seppala, H. Antelmann, H. Boer, S. Taira, H. Savilahti, M. Hecker, M. Vihinen, M. Sarvas, V.P. Kontinen, Structure-function analysis of PrsA reveals roles for the parvulin-like and flanking N- and C-terminal domains in protein folding and secretion in *Bacillus subtilis*, J. Biol. Chem., 279 (2004) 19302–19314.
[334] M. Jacobs, J.B. Andersen, V. Kontinen, M. Sarvas, *Bacillus subtilis* PrsA is required *in vivo* as an extracytoplasmic chaperone for secretion of active enzymes synthesized either with or without pro-sequences, Mol. Microbiol., 8 (1993) 957–966.
[335] O. Heikkinen, R. Seppala, H. Tossavainen, S. Heikkinen, H. Koskela, P. Permi, I. Kilpelainen, Solution structure of the parvulin-type PPIase domain of *Staphylococcus aureus* PrsA–implications for the catalytic mechanism of parvulins, BMC Struct. Biol., 9 (2009) 17.
[336] H. Tossavainen, P. Permi, S.L. Purhonen, M. Sarvas, I. Kilpelainen, R. Seppala, NMR solution structure and characterization of substrate binding site of the PPIase domain of PrsA protein from *Bacillus subtilis*, FEBS Lett., 580 (2006) 1822–1826.
[337] R.P. Jakob, J.R. Koch, B.M. Burmann, P.A. Schmidpeter, M. Hunkeler, S. Hiller, F.X. Schmid, T. Maier, Dimeric structure of the bacterial extracellular foldase PrsA, J. Biol. Chem., 290 (2015) 3278–3292.
[338] C.T. Webb, M.A. Gorman, M. Lazarou, M.T. Ryan, J.M. Gulbis, Crystal structure of the mitochondrial chaperone TIM9*10 reveals a six-bladed α-propeller, Mol. Cell, 21 (2006) 123–133.
[339] K.N. Beverly, M.R. Sawaya, E. Schmid, C.M. Koehler, The Tim8-Tim13 complex has multiple substrate binding sites and binds cooperatively to Tim23, J. Mol. Biol., 382 (2008) 1144–1156.
[340] H. Lu, A.P. Golovanov, F. Alcock, J.G. Grossmann, S. Allen, L.Y. Lian, K. Tokatlidis, The structural basis of the TIM10 chaperone assembly, J. Biol. Chem., 279 (2004) 18959–18966.
[341] M.S. Paget, M.J. Buttner, Thiol-based regulatory switches, Annu. Rev. Genet., 37 (2003) 91–121.
[342] U. Jakob, W. Muse, M. Eser, J.C. Bardwell, Chaperone activity with a redox switch, Cell, 96 (1999) 341–352.
[343] P.C. Graf, M. Martinez-Yamout, S. VanHaerents, H. Lilie, H.J. Dyson, U. Jakob, Activation of the redox-regulated chaperone Hsp33 by domain unfolding, J. Biol. Chem., 279 (2004) 20529–20538.
[344] S.J. Kim, D.G. Jeong, S.W. Chi, J.S. Lee, S.E. Ryu, Crystal structure of proteolytic fragments of the redox-sensitive Hsp33 with constitutive chaperone activity, Nat. Struct. Biol., 8 (2001) 459–466.
[345] Y.S. Lee, K.S. Ryu, S.J. Kim, H.S. Ko, D.W. Sim, Y.H. Jeon, E.H. Kim, W.S. Choi, H.S. Won, Verification of the interdomain contact site in the inactive monomer, and the domain-swapped fold in the active dimer of Hsp33 in solution, FEBS Lett., 586 (2012) 411–415.
[346] H.S. Won, L.Y. Low, R.D. Guzman, M. Martinez-Yamout, U. Jakob, H.J. Dyson, The zinc-dependent redox switch domain of the chaperone Hsp33 has a novel fold, J. Mol. Biol., 341 (2004) 893–899.
[347] Y. Ishida, K. Nagata, Hsp47 as a collagen-specific molecular chaperone, Methods Enzymol., 499 (2011) 167–182.
[348] K. Nagata, Hsp47 as a collagen-specific molecular chaperone: function and expression in normal mouse development, Semin. Cell Dev. Biol., 14 (2003) 275–282.

[349] M. Yagi-Utsumi, S. Yoshikawa, Y. Yamaguchi, Y. Nishi, E. Kurimoto, Y. Ishida, T. Homma, J. Hoseki, Y. Nishikawa, T. Koide, K. Nagata, K. Kato, NMR and mutational identification of the collagen-binding site of the chaperone Hsp47, PLoS One, 7 (2012) e45930.
[350] J. Monod, J.P. Changeux, F. Jacob, Allosteric proteins and cellular control systems, J. Mol. Biol., 6 (1963) 306–329.
[351] P. Csermely, R. Palotai, R. Nussinov, Induced fit, conformational selection and independent dynamic segments: an extended view of binding events, Trends Biochem. Sci., 35 (2010) 539–546.
[352] R.G. Smock, L.M. Gierasch, Sending signals dynamically, Science, 324 (2009) 198–203.
[353] A. del Sol, C.J. Tsai, B. Ma, R. Nussinov, The origin of allosteric functional modulation: multiple pre-existing pathways, Structure, 17 (2009) 1042–1050.
[354] M.P. Mayer, H. Schröder, S. Rüdiger, K. Paal, T. Laufen, B. Bukau, Multistep mechanism of substrate binding determines chaperone activity of Hsp70, Nat. Struct. Biol., 7 (2000) 586–593.
[355] V. Fernandez-Saiz, F. Moro, J.M. Arizmendi, S.P. Acebron, A. Muga, Ionic contacts at DnaK substrate binding domain involved in the allosteric regulation of lid dynamics, J. Biol. Chem., 281 (2006) 7479–7488.
[356] F. Moro, V. Fernandez-Saiz, A. Muga, The lid subdomain of DnaK is required for the stabilization of the substrate-binding site, J. Biol. Chem., 279 (2004) 19600–19606.
[357] S.J. Yoo, J.H. Seol, D.H. Shin, M. Rohrwild, M.S. Kang, K. Tanaka, A.L. Goldberg, C.H. Chung, Purification and characterization of the heat shock proteins HslV and HslU that form a new ATP-dependent protease in *Escherichia coli*, J. Biol. Chem., 271 (1996) 14035–14040.
[358] X. Zhu, X. Zhao, W.F. Burkholder, A. Gragerov, C.M. Ogata, M.E. Gottesman, W.A. Hendrickson, Structural analysis of substrate binding by the molecular chaperone DnaK, Science, 272 (1996) 1606–1614.
[359] H. Wang, A.V. Kurochkin, Y. Pang, W. Hu, G.C. Flynn, E.R. Zuiderweg, NMR solution structure of the 21 kDa chaperone protein DnaK substrate binding domain: a preview of chaperone-protein interaction, Biochemistry, 37 (1998) 7929–7940.
[360] S.Y. Stevens, S. Sanker, C. Kent, E.R. Zuiderweg, Delineation of the allosteric mechanism of a cytidylyltransferase exhibiting negative cooperativity, Nat. Struct. Biol., 8 (2001) 947–952.
[361] T.E. Gray, J. Eder, M. Bycroft, A.G. Day, A.R. Fersht, Refolding of barnase mutants and pro-barnase in the presence and absence of GroEL, EMBO J., 12 (1993) 4145–4150.
[362] T.E. Gray, A.R. Fersht, Refolding of barnase in the presence of GroE, J. Mol. Biol., 232 (1993) 1197–1207.
[363] F.J. Corrales, A.R. Fersht, The folding of GroEL-bound barnase as a model for chaperonin-mediated protein folding, Proc. Natl. Acad. Sci. USA, 92 (1995) 5326–5330.
[364] A.A. Lilly, J.M. Crane, L.L. Randall, Export chaperone SecB uses one surface of interaction for diverse unfolded polypeptide ligands, Protein Sci., 18 (2009) 1860–1868.
[365] K.A. Krukenberg, U.M. Böttcher, D.R. Southworth, D.A. Agard, Grp94, the endoplasmic reticulum Hsp90, has a similar solution conformation to cytosolic Hsp90 in the absence of nucleotide, Protein Sci., 18 (2009) 1815–1827.
[366] K.A. Krukenberg, F. Förster, L.M. Rice, A. Šali, D.A. Agard, Multiple conformations of *E. coli* Hsp90 in solution: insights into the conformational dynamics of Hsp90, Structure, 16 (2008) 755–765.

[367] J.H. Viles, D. Donne, G. Kroon, S.B. Prusiner, F.E. Cohen, H.J. Dyson, P.E. Wright, Local structural plasticity of the prion protein. Analysis of NMR relaxation dynamics, Biochemistry, 40 (2001) 2743–2753.
[368] R.R. Ernst, G. Bodenhausen, A. Wokaun, Principles of Nuclear Magnetic Resonance in One and Two Dimensions, Clarendon, Oxford, 1987.
[369] Y. Papanikolau, M. Papadovasilaki, R.B. Ravelli, A.A. McCarthy, S. Cusack, A. Economou, K. Petratos, Structure of dimeric SecA, the *Escherichia coli* preprotein translocase motor, J. Mol. Biol., 366 (2007) 1545–1557.
[370] M. Carroni, E. Kummer, Y. Oguchi, P. Wendler, D.K. Clare, I. Sinning, J. Kopp, A. Mogk, B. Bukau, H.R. Saibil, Head-to-tail interactions of the coiled-coil domains regulate ClpB activity and cooperation with Hsp70 in protein disaggregation, eLife, 3 (2014) e02481.
[371] R. Kityk, J. Kopp, I. Sinning, M.P. Mayer, Structure and dynamics of the ATP-bound open conformation of Hsp70 chaperones, Mol. Cell, 48 (2012) 863–874.
[372] J. Zimmer, Y.S. Nam, T.A. Rapoport, Structure of a complex of the ATPase SecA and the protein-translocation channel, Nature, 455 (2008) 936–943.
[373] A. Hoffmann, B. Bukau, G. Kramer, Structure and function of the molecular chaperone trigger factor, Biochim. Biophys. Acta, 1803 (2010) 650–661.
[374] J. Serek, G. Bauer-Manz, G. Struhalla, L. van den Berg, D. Kiefer, R. Dalbey, A. Kuhn, *Escherichia coli* YidC is a membrane insertase for Sec-independent proteins, EMBO J., 23 (2004) 294–301.

Glossary

A-Skp: Selectively alanine-labeled Skp
AAA+: ATPases associated with diverse cellular activities
Aβ: Amyloid beta
ADP: Adenosine diphosphate
Aha1: Activator of Hsp90 ATPase protein 1
ATP: Adenosine triphosphate
ATPase: ATP hydrolase
Bag1: BAG family molecular chaperone regulator 1
BamA: β-barrel assembly machinery
CD: Circular dichroism
Clp: ATP-dependent Clp protease
CP: core particle
CRINEPT: cross-correlated relaxation-enhanced polarization transfer
CRIPT: cross-correlated relaxation-induced polarization transfer
CSP: Chemical shift perturbation
DEST: Dark state exchange saturation transfer
DHFR: Dihydrofolate reductase
DnaJ: Chaperone protein DnaJ
DnaK: Chaperone protein DnaK
DNP: Dynamic nuclear polarization
DOSY: Diffusion-ordered NMR spectroscopy
EM: Electron microscopy
EPR: Electron paramagnetic resonance
FhaC: Filamentous hemagglutinin transporter
FkpA: FKBP-type peptidyl-prolyl cis-trans isomerase
FKBP: FK506 binding protein
FROSTY: Freezing rotational diffusion of protein solutions at low temperature and high viscosity
GroEL: Chaperone protein GroEL
GroES: Chaperone protein GroES
GrpE: Hsp70 cofactor GrpE
H/D-exchange: hydrogen/deuterium exchange
Hdj1: DnaJ homolog subfamily B member 1
Hsc70: Heat shock cognate 70 kDa protein
HslU: ATP-dependent protease ATPase subunit HslU
HslV: ATP-dependent protease subunit HslV
Hsp: Heat shock protein
HSQC: Heteronuclear single quantum coherence
ILV-: Selectively isoleucine, leucine and valine labeled
INEPT: Insensitive nuclei enhanced by polarization transfer
IRA: Intramolecular regulator of ATP hydrolysis
ITC: Isothermal titration calorimetry
L6: Extracellular loop 6 of the Omp85 protein family

LamB: Maltoporin
MALS: Multi-angle light scattering
MAS: Magic angle spinning
M-domain: Middle domain
MKT-077: 1-Ethyl-2-[[3-ethyl-5-(3-methyl-2(3H)-benzothiazolylidene)-4-oxo-2-thiazolidinylidene]methyl]-pyridinium chloride
N-domain: N-terminal domain
NEF: Nucleotide exchange factor
NMR: Nuclear magnetic resonance
NOE: Nuclear Overhauser effect
Omp: Outer membrane protein
Omp85: Outer membrane protein family Omp85
OmpA: Outer membrane protein A
p23: Co-chaperone of Hsp90
p53: Cellular tumor antigen p53
PBD: Preprotein-binding domain
PCS: Pseudo contact shift
PDB: Protein data bank
PhoA: Alkaline phosphatase IV
POTRA: Polypeptide transport associated domain
PPD: Peptidyl-prolyl-isomerase domain
ppiD: Peptidyl-prolyl cis-trans isomerase D
ppm: Parts per million
PRE: Paramagnetic relaxation enhancement
PrsA: Foldase protein PrsA
RBD: Ribosome binding domain
RDC: Residual dipolar coupling
RLA: R-lactalbumin
RNA: Ribonucleic acid
SAXS: Small angle X-ray scattering
SBD: Substrate binding domain
SecA: Protein translocase subunit SecA
SecB: Protein-export protein SecB
SecYEG: Protein translocase SecYEG
sHsp: Small heat shock protein
Skp: Chaperone protein Skp
SR1: Single-ring GroEL
ssNMR: Solid state NMR
STD: Saturation transfer difference
Sup35: Yeast prion protein Sup35
SurA: Survival factor A
Tah1: TPR repeat-containing protein associated with Hsp90
TamA: Translocation and assembly module
Tau: Microtubule-associated protein tau
TF: Trigger factor
Tim: Mitochondrial import inner membrane translocase subunit (Tim8, Tim9, Tim10, Tim13)
Tom: Translocase of the outer mitochondrial membrane

Tom40: Translocase of the outer mitochondrial membrane 40kDa subunit
TRiC: TCP-1 ring complex
tOmpA: Transmembrane domain of OmpA
Toc75: 75 kDa translocon at the outer envelope membrane of chloroplasts
trNOE: Transfer NOE
TROSY: Transverse relaxation optimized spectroscopy
YidC: Membrane protein insertase YidC
ZBD: Zinc-binding domain